© 2022. Published by The Company of Biologists Ltd | Development (2022) 149, dev200353. doi:10.1242/dev.200353

HUMAN DEVELOPMENT

RESEARCH ARTICLE

Laminin 511 and WNT signalling sustain prolonged expansion of hiPSC-derived hippocampal progenitors

Keagan Dunville[1], Fabrizio Tonelli[1], Elena Novelli[2], Azzurra Codino[3], Verediana Massa[2], Anna Maria Frontino[1], Silvia Galfrè[4], Francesca Biondi[2], Stefano Gustincich[3], Matteo Caleo[2,‡], Luca Pandolfini[3,*], Claudia Alia[2,*] and Federico Cremisi[1,*,§]

ABSTRACT

Using the timely re-activation of WNT signalling in neuralizing human induced pluripotent stem cells (hiPSCs), we have produced neural progenitor cells with a gene expression profile typical of human embryonic dentate gyrus (DG) cells. Notably, in addition to continuous WNT signalling, a specific laminin isoform is crucial to prolonging the neural stem state and to extending progenitor cell proliferation for over 200 days *in vitro*. Laminin 511 is indeed specifically required to support proliferation and to inhibit differentiation of hippocampal progenitor cells for extended time periods when compared with a number of different laminin isoforms assayed. Global gene expression profiles of these cells suggest that a niche of laminin 511 and WNT signalling is sufficient to maintain their capability to undergo typical hippocampal neurogenesis. Moreover, laminin 511 signalling sustains the expression of a set of genes responsible for the maintenance of a hippocampal neurogenic niche. Finally, xenograft of human DG progenitors into the DG of adult immunosuppressed host mice produces efficient integration of neurons that innervate CA3 layer cells spanning the same area of endogenous hippocampal neuron synapses.

KEY WORDS: Hippocampus, Neurogenesis, Neural progenitor cell, WNT, Notch, hiPSC, Neurogenetic niche, Cell transplantation, Zbtb20, Laminin 511

INTRODUCTION

Although neurogenesis is ubiquitous throughout embryonic stages, it is also known to persist in the subventricular and subgranular zones postnatally, and has been extensively studied since the discovery of newborn neurons in adult rodents (Altman and Das, 1965). These regions, the ventral telencephalic subventricular zone (SVZ) and the dentate gyrus subgranular zone (SGZ), develop tangentially to the angiogenic niches in vertebrates and are attributed with newborn neurons throughout the rostral migratory system and the hippocampus, respectively (Palmer et al., 2000; Pencea et al., 2001). In addition, adult neurogenesis in the striatum has also been reported (Inta et al., 2015). However, adult neurogenesis has been primarily studied in the hippocampus because of its involvement in age-dependent cognitive decline (Bettio et al., 2017). Adult hippocampal neurogenesis is found across several model organisms, including mouse, non-human primates and humans (Charvet and Finlay, 2018). Induction of hippocampal neurogenesis has been associated with exercise (van Praag et al., 2005), acute stress (Brandhorst et al., 2015), the insulin pathway (Åberg et al., 2000), stimulation with parvalbumin (Song et al., 2013), astrocytic glutamate release (Asrican et al., 2020) and Notch inhibition (Lugert et al., 2010). Hippocampal neurogenesis persists throughout adulthood in higher mammalian vertebrates and has been associated with *de novo* working memory formation (Ming and Song, 2011). Studying neurogenesis in the human hippocampus has proved especially challenging. Ethical implications regarding human hippocampal samples have made human hippocampus specimens difficult to obtain. The lack of non-invasive methods restricts investigation even further (Lester et al., 2017). Most hippocampal neurogenesis studies have therefore relied on rodent models, providing insight into developmental signals necessary for hippocampal generation (Grove et al., 1998), molecular actuators of neural progenitor cell (NPC) exit from the cell cycle (Asrican et al., 2020; Song et al., 2013) and neurogenic-dependent memory consolidation (Berdugo-Vega et al., 2020).

The role of extrinsic cues in establishing and maintaining the human hippocampal neurogenetic niche remains unknown. Evidence identifies Wnt signalling as the main extrinsic cue for hippocampal identity specification. A local Wnt reservoir in the cortical hem drives early hippocampal development until E9.5 in mice (Grove et al., 1998), which contributes to further hippocampal differentiation (Machon et al., 2007). Cortical hem-derived Wnt3a activates canonical β-catenin signalling and is thought to serve as the hippocampal organizer (Lee et al., 2000; Rosenthal et al., 2012). It is also evident that Wnt signalling is necessary to further propagate hippocampal formation because lymphoid enhancing-binding factor 1 and LIM homeobox-binding domain proteins, which are downstream transcription factors of β-catenin pathway, are upregulated at E14.5 and E16.5 in mice (Abellán et al., 2014). Additional signalling is required for the establishment and maintenance of hippocampal neurogenesis. BMP maintains stem cell proliferation in the embryo, while it promotes quiescence to prevent stem cell exhaustion in the adult brain (Urbán and Guillemot, 2014). Moreover, SHH signalling controls the establishment of the quiescent neural stem cell (NSC) pool (Noguchi et al., 2019) while Notch signalling regulates NPC number during development and maintains a reservoir of undifferentiated cells in adulthood (Ables et al., 2010). Among the many factors contributing to hippocampal neurogenesis, involvement of extrinsic cues from the extracellular matrix has been neglected. Laminin regulates neural progenitor cell survival, proliferation and

[1]Laboratorio di Biologia, Scuola Normale Superiore, Pisa, 56126, Italy. [2]Istituto di Neuroscienze, Consiglio Nazionale delle Ricerche, Pisa, 56124, Italy. [3]Center for Human Technologies, Central RNA Lab, Istituto Italiano di Tecnologia, Genova, 16152, Italy. [4]Department of Biology and Biotechnologies 'Charles Darwin', Università La Sapienza, Roma, 00185, Italy.
*These authors contributed equally to this work
‡Deceased April 13 2022

§Author for correspondence (federico.cremisi@sns.it)

F.C., 0000-0003-4925-2703

Handling Editor: Paola Arlotta
Received 12 November 2021; Accepted 8 August 2022

Development (2022) 149, dev200353. doi:10.1242/dev.200353

differentiation by the developmentally regulated formation of laminin-rich structures, called fractones (Long and Huttner, 2019). Laminin α5 chain expressed by fractone bulbs continues to regulate neurogenesis in the SVZ (Nascimento et al., 2018) and promotes survival, network formation and functional development of human pluripotent stem cell-derived neurons *in vitro* (Hyysalo et al., 2017). Nonetheless, the role of laminins in the hippocampal neurogenetic niche has not yet been investigated.

Previous protocols describe general hippocampal identity differentiation from mouse embryonic stem cells (mESCs) (Terrigno et al., 2018), human embryonic stem cells (hESCS) (Sakaguchi et al., 2015; Yu et al., 2014b), CA3 (Sarkar et al., 2018) or dentate gyrus (DG) cells from human induced pluripotent stem cells (hiPSCs) (Yu et al., 2014a). However, the effect of different extrinsic cues on the maintenance of a neurogenic niche *in vitro* and the global gene expression profiles of human hippocampal progenitors differentiating in culture were not investigated. We developed a novel protocol to differentiate hippocampal NPCs from hiPSCs via a known WNT actuator and GSK-3b inhibitor: CHIR99021 (Naujok et al., 2014). We accurately compared the molecular nature of the cells produced by our protocol with that of human cells from embryonic hippocampus and from other brain regions by global transcriptomics; our analysis revealed a bona fide hippocampal NPC identity. The generation of hippocampal NPCs allowed us to investigate the extrinsic cues of the hippocampal neurogenetic niche. We first dissected the relative roles of WNT and Notch signalling in establishing a hippocampal identity or controlling neuronal differentiation. We then focused on the laminin composition of a niche allowing the maintenance of hippocampal neurogenesis. Notwithstanding prolonged expansion (>200 days), the hippocampal NPCs cultured on laminin α5β1γ1 (laminin 511) retained the capacity to proliferate neurogenically. Indeed, we found that laminin 511 supports adhesion and cell cycle progression of dividing hippocampal progenitors. The differentiation capability of both young and older NPC populations was confirmed by xenografting into the dentate gyrus of wild-type mice, wherein both groups of differentiating neurons established synapses within their respective hosts with comparable efficiency. Our findings indicate that WNT signalling and laminin 511 are required for the maintenance of a niche supporting human hippocampal neurogenesis.

RESULTS

WNT signalling by GSK-3β inhibition induces a hippocampal-like neuronal identity in hiPSC cultures

We established a protocol to derive hippocampal neural precursor cells from hiPCcs. To obtain a general neural telencephalic differentiation of hiPSCs, we first inhibited WNT, BMP and TGFβ signalling (Martins et al., 2021; Shi et al., 2012a,b). WNT-, BMP- and TGFβ-inhibited (WiBiTi) cells from day 0 of *in vitro* differentiation (DIV0) to DIV12 were used as starting point to assay the ability of WNT re-activation to induce the expression of key markers of hippocampal positional identity (hippocampal identity markers) (Fig. 1A). To induce a hippocampal identity, we adapted two protocols (Sakaguchi et al., 2015; Terrigno et al., 2018) that use the GSK-3β inhibitor CHIR99201 (CHIR) to activate WNT signalling. We thus re-activated WNT signalling in early telencephalic progenitor cells by CHIR at different times of culture, looking for the optimal time window of cell competence for acquiring a hippocampal identity (Fig. 1A). We re-activated WNT signalling from DIV12, DIV16, DIV20 or DIV24 for either 8 or 12 days (Fig. 1A). We then assessed hippocampal identity markers by qRT-PCR, including *EMX2*, *FOXG1*, *PROX1*, *WNT8A* and *ZBTB20* (Fig. 1B). We found that only CHIR treatment starting from DIV16 and lasting 12 days (W16-28) induced significant upregulation of *PROX1*, *WNT8A* and *ZBTB20* compared with control cells (WiBiTi treatment from DIV0 to DIV14 and no treatment from DIV14 to DIV36).

The identity of W16-28-treated cells (referred to here as CHIR cells) was first assessed by RNA-seq analysis. At the transition between DIV0 (hIPSCs) and DIV28 CHIR cells, 1813 and 1517 genes were significantly up- and downregulated, respectively (Fig. 1C). The analysis of Gene Ontology (GO) enrichment of the differentially expressed (DE) genes highlighted many terms related to developmental processes, neural differentiation and anatomical identity, in line with the acquisition of a specific neuronal cell identity of hiPSCs (Table S1). To further refine the identity analysis of CHIR cells, we focused on the expression of a panel of 59 hippocampal identity markers established from the literature (Table S2) and found that most of them were upregulated in CHIR cells at DIV28 when compared with hIPSCs (Fig. 1D). Moreover, we compared the expression of these markers between DIV28 CHIR cells and human embryonic visual cortex, hippocampus, dorsal thalamus, striatum and cerebellum at 12 postconceptional weeks (PCWs), as reported by the Allen Brain Atlas (ABA) (Colantuoni et al., 2011). Hierarchical clustering analysis (Fig. 1E) indicates that the expression of this cell marker panel is more similar between DIV28 CHIR cells and hippocampus than between DIV28 CHIR cells and the other encephalic regions.

When assaying by immunocytodetection (ICD), the expression of the hippocampal identity markers ZBTB20 (Nielsen et al., 2014; Sakaguchi et al., 2015), PROX1 (Lavado et al., 2010) and BCL11B (Simon et al., 2012), and the marker of the neurogenic niche of the dentate gyrus DCX (Knoth et al., 2010) at DIV33 we found a significant increase in CHIR cells compared with cultures in which WNT signalling was continuously inhibited until DIV28 (WiBiTi) (Martins et al., 2021) (Fig. 1F). Moreover, CHIR cultures showed more KI67-positive dividing progenitors than WiBiTi cultures, indicating proliferative differences between the two types of cell progenitors.

Both WiBiTi and CHIR cells spontaneously differentiated on natural mouse laminin (msl) and survived until DIV 60, expressing similar levels of neuronal markers (βIII-tubulin, N-acetylated tubulin, NEUN, MAP2) and pallial markers (FOXG1 and PAX6) (Fig. S1A,B). Interestingly, CHIR cells plated onto mESC-derived hippocampal cultures (Terrigno et al., 2018) could survive longer and were able to generate KI67-positive dividing progenitors, DCX-positive precursors and ZBTB20-positive cells until DIV70 (Fig. S1C-E). In these conditions, the Notch pathway-inhibitor DAPT significantly decreased the proportion of $KI67^+$ and DCX^+ NPCs (Fig. S1E), and allowed the expression of MAP2, a marker of differentiated neurons (Fig. S1D). Altogether, our observations indicate that the timely treatment with CHIR from DIV16 to DIV28 generated genuine pallial NPCs with competence to differentiate as neurons and a gene expression profile typical of human embryonic hippocampal cells.

WNT signalling specifically affects the identity of telencephalic neural progenitor cells generated by hiPSCs

The exact mechanism of WNT signalling in establishing a hippocampal identity in telencephalic progenitor cells is not completely elucidated, although it is known that Notch signalling is fundamental to maintaining hippocampal neurogenesis in both embryonic and mature hippocampus (Imayoshi et al., 2010). Aiming to discriminate between WNT and Notch signalling

Development (2022) 149, dev200353. doi:10.1242/dev.200353

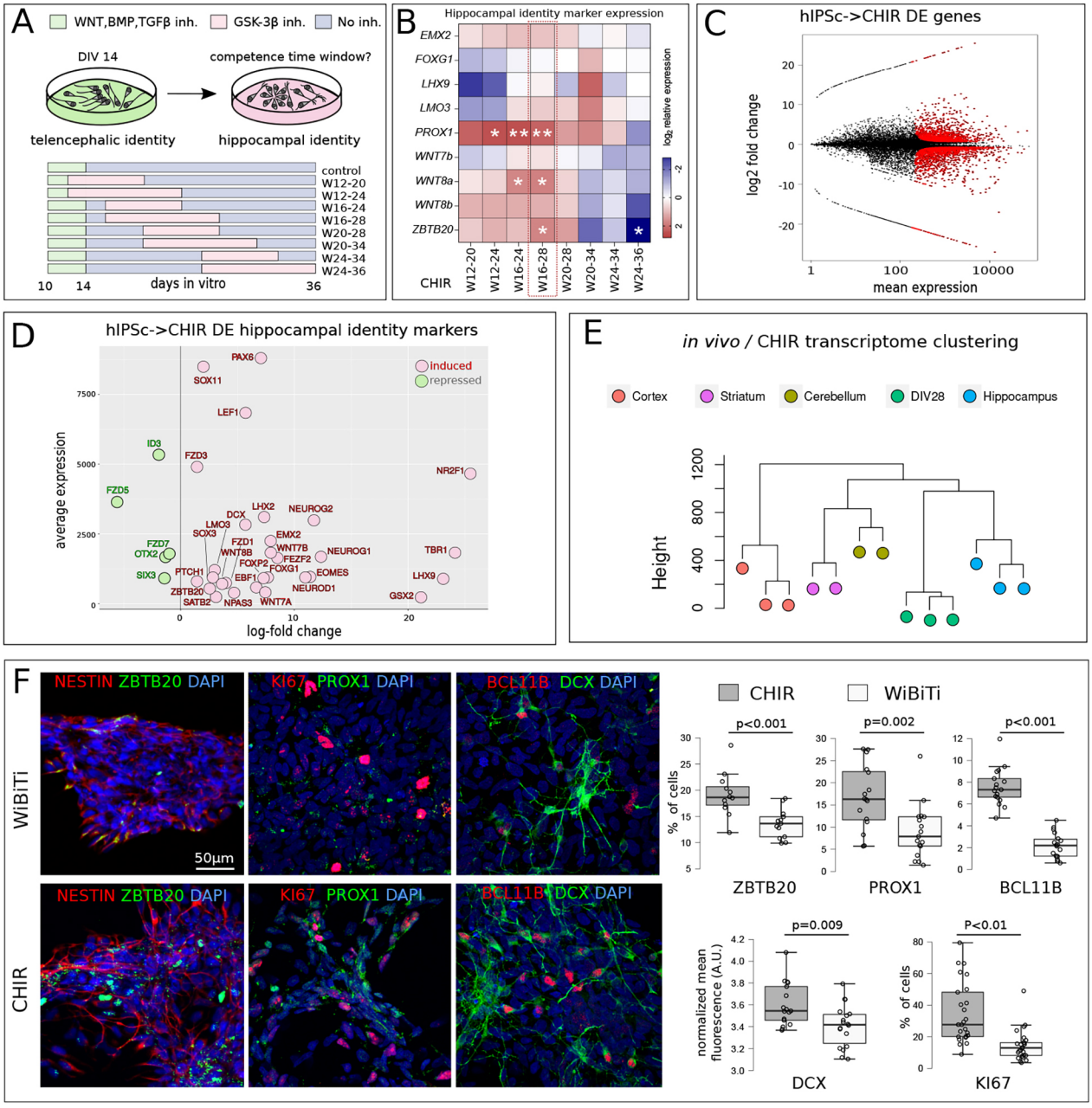

Fig. 1. GSK3β inhibition by CHIR induces a hippocampal-like neuronal identity in hiPSC cultures. (A) Experimental schematic outlining the timing of drug addition and withdrawal starting from DIV10 until DIV36. WNT signalling (W) was activated by GSK-3β inhibition (inh) in the different time windows indicated by the numbers, which indicate the day of *in vitro* differentiation (DIV). (B) qRT-PCR analysis of hippocampal identity markers including *EMX2*, *FOXG1*, *LXH9*, *LMO3*, *PROX1*, *WNT7B*, *WNT8A*, *WNT8B* and *ZBTB20* in $n=3$ biological replicates at DIV36. *PROX1*, *WNT8A* and *ZBTB20* were positively and significantly upregulated in CHIR (W16-28) cells in comparison with control cells in which WNT, BMP and TGFβ were inhibited from DIV0 to DIV14; $^{*}P<0.05$, $^{**}P<0.01$, as analysed by two-way ANOVA using Sidak-Holm correction. (C) Plot of differentially expressed (DE) genes of CHIR (W16-28) cells (thereafter known as CHIR cells) when compared with hiPSCs ($n=3$ biological replicates). Cells were analysed at the end of the treatment (DIV28). Red dots indicate DE genes as found by NOIseq (q>0.8). (D) Selected hippocampal identity markers (Table S1) differentially expressed between DIV28 CHIR cells and hiPSCs (NOIseq, q>08). (E) Hierarchical clustering of selected hippocampal identity markers (see Table S1) as evaluated using $n=3$ biological replicates of bulk RNA-seq using DIV28 CHIR cells in comparison with the Allen Brain Atlas (ABA) regions indicated in labels at 12 PCW ($n=3$ each). (F) CHIR cells compared with cortical WiBiTi cells at DIV33 ($n=3$ biological replicates). WiBiTi cells were inhibited from DIV0 to DIV28 to acquire cortical identity (Martins et al., 2021). DIV28 WiBiTi and CHIR cells were seeded on mouse laminin (msl) and cultured in minimal medium until DIV33. Immunofluorescence shows immunocytodetection (ICD) of markers of hippocampal identity (ZBTB20, PROX1 and BCL11B), dividing progenitors (KI67) and hippocampal post-mitotic precursor cells (DCX). Cell count analysis was performed using a Mann–Whitney nonparametric test on $n=3$ biological replicates. In the box and whisker plots, the horizontal line indicates the median, the upper and lower edges of the boxes represent the bounds of the interquartile interval, and the whiskers represent the 99% confidence interval.

effects in our cultures, we induced neuronal differentiation using the γ-secretase inhibitor DAPT in cultures with or without CHIR treatment. Principal component analysis (PCA) of the transcriptomes of different cultures (Fig. 2A) indicates that the majority of gene expression variability detected by the first component (68.24%) accounts for the difference in DAPT,

Development (2022) 149, dev200353. doi:10.1242/dev.200353

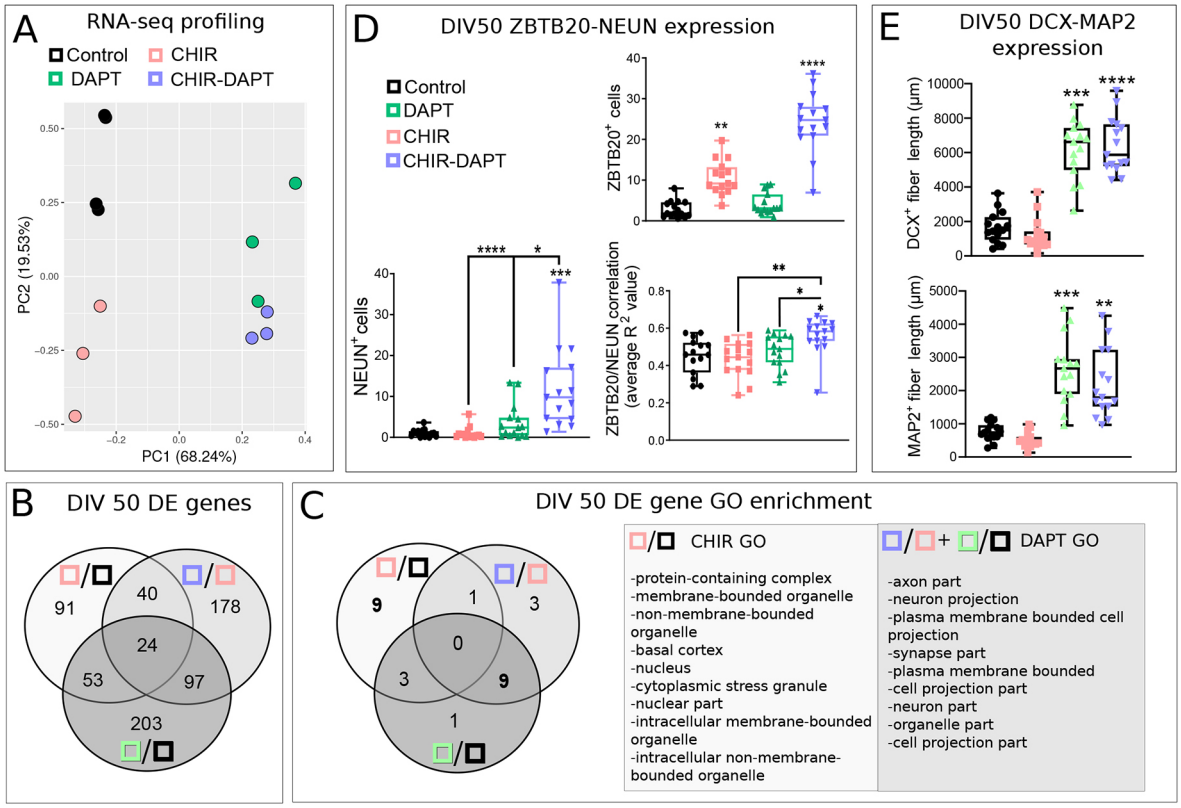

Fig. 2. The identity of neuralized hiPSCs is differently affected by WNT and Notch signalling. (A-E) DIV40 CHIR cells were plated on msl and cultured until DIV50 in minimal medium (Control), or treated at DIV46 for two days with CHIR, DAPT or CHIR-DAPT. Inhibitors were removed after 2 days and cells were maintained in minimal medium for another 2 days before analysis; *n*=3 biological replicates for each condition. (A) RNA-seq PCA (obtained by R Cran prcomp function) of DIV50 cultures treated as indicated by labels. (B,C) Venn diagrams reporting the intersection of DE genes (B) and GO enriched terms of DE genes (C), between the culture conditions indicated by labels as in A. DE genes were determined by NOIseq (q>0.8). (D) Percentage of DIV50 cells as in A analysed by NEUN, ZBTB20, DCX and MAP2 imaging. Average Pearson correlation between ZBTB20 and NEUN indicates the degree of overlapping signal of the two markers in CHIR/DAPT compared with all groups. (E) Experiments as in D to measure the total length of cell processes positive for DCX and MAP2. Statistical analyses were performed by one-way ANOVA, post-hoc Kruskal–Wallis test; asterisks above plotted values indicate comparison against control, whereas asterisks above solid black bars indicate comparison between groups. **P*<0.05, ***P*<0.01, ****P*<0.001, *****P*<0.0001. In the box and whisker plots, the horizontal line indicates the median, the upper and lower edges of the boxes represent the bounds of the interquartile interval, and the whiskers represent the 99% confidence interval.

whereas CHIR differentiates the expression profiles at a lower extent along the second component (19.53%). The two treatments, alone or in combination, induce the expression of sets of genes that are either specific for a given condition, or common between two conditions (Fig. 2B). However, the gene ontology enrichment analysis of these sets reveals that genes expressed in CHIR-treated cells are very different from those of DAPT-treated cells, indicating that the two treatments affect different processes, with those induced by DAPT clearly involving the neuralization of cells (Fig. 2C).

We aimed to identify a single specific hippocampal marker of both progenitor and differentiating cells to assay the effects of WNT and Notch signalling. *Zbtb20* suppresses the acquisition of an isocortical fate during archicortical neurogenesis (Nielsen et al., 2014), playing a key role in the specification of the CA1 field identity and in the postnatal survival of hippocampal neurons (Xie et al., 2010). These features make it a good candidate as a marker for hippocampal identity. To investigate the potential relationship between *Zbtb20* and hippocampal neurogenesis, we analysed scRNA-seq of mouse hippocampal data sets at timepoints E16.5, P0, P5 and P23 (Fig. S2). Like previous findings (Mitchelmore et al., 2002), *Zbtb20* is expressed in a large fraction of mouse hippocampal cells at E16.5 but it restricts its expression in developing (P0 and P5) and mature (P23) hippocampus, showing some degree of co-expression with *Dcx* (Fig. S2A). We took advantage of a scRNA-seq analysis method, COTAN (Galfrè et al., 2021), to evaluate the co-expression of *Zbtb20* with respect to distinct selected markers of NPCs, hippocampal cell identity and neuronal differentiation (Fig. S2B). We found that *Zbtb20* embryonic expression correlates with many markers of early hippocampal neurogenesis but it is not restricted to a specific step of cell differentiation.

We therefore compared the expression of ZBTB20 to the expression of nestin and NEUN 48 h after different combinations of DAPT and CHIR treatment (Fig. S3A, Fig. 2D,E). Although nestin was not downregulated by DAPT, NEUN- and ZBTB20-positive cell ratio changed between treatments. ZBTB20 was most upregulated in CHIR-DAPT cultures, followed by CHIR culture compared with control (Fig. 2D). Instead, only CHIR/DAPT treatment significantly increased the number of NEUN-positive cells (Fig. 2D). This observation is in agreement with the role of WNT signalling in inducing a hippocampal identity rather than merely supporting neurogenesis. According to the inhibitory effect of Notch signalling on neurogenesis, DAPT treatment, both alone and together with CHIR treatment, induced outgrowth of DCX^+ and $MAP2^+$ fibres (Fig. S3B, Fig. 2E).

Development (2022) 149, dev200353. doi:10.1242/dev.200353

Specific laminin substrate and constitutive CHIR treatment prolongs proliferation of hiPSC-derived hippocampal progenitors

In addition to intrinsic signals, we looked for extrinsic cues possibly supporting the hippocampal neurogenic niche. Among the most likely candidates, laminins play a key role (see Introduction). To model prolonged neurogenesis, we theorized that the laminin substrate could be actively involved in maintaining the neural stem niche but that removal from that niche would stimulate cell cycle exit. We hypothesized that distinct types of laminin exist, supporting proliferation or differentiation of NPCs (laminin P and laminin D, respectively; Fig. 3A). We chose to focus on laminin isoforms either expressed in the neural ECM landscape or previously assessed in literature. To functionally assay distinct laminins, we plated DIV28 CHIR cells on glass coated with poly-l-ornithine and one of the following recombinant laminin substrates: control laminin [purified mouse laminin (msl), composed of α1,β1,γ1 subunits], laminin 511 (α5,β1,γ1), laminin 121 (α1,β2,γ1), laminin

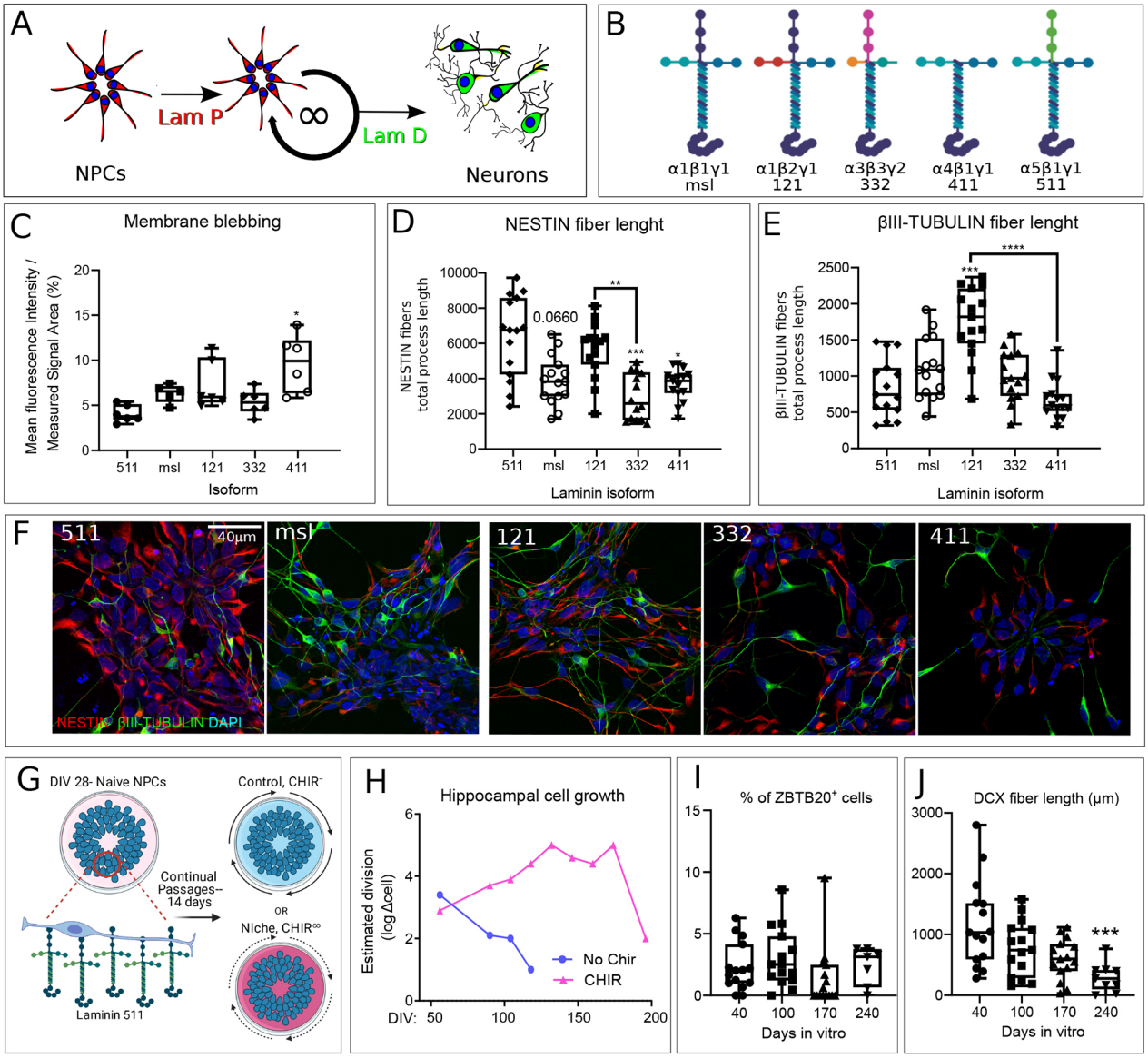

Fig. 3. Laminin isoform type is crucial to prolonging neural stem state and extends hippocampal NSC proliferation for over 200 days *in vitro*. (A) Schematic anticipating the role of different laminins (LAM P, laminin of proliferation; LAM D, laminin of differentiation) in supporting neural progenitor cell (NPC) self-renewal or neuronal differentiation. (B) Laminin isoforms and their structural representation. msl, mouse laminin. (C) DIV28 CHIR cells (NPCs) were seeded on the indicated laminin isoforms and maintained in minimal medium for 5 days before fixation at DIV33 (n=3 biological replicates). Membrane blebbing in the different culture conditions was evaluated by the analysis of membrane permeabilization calculated as TOTO-3 fluorescence/Hoechst nuclear area. Data were analysed with one-way ANOVA and post-hoc Kruskal–Wallis tests; n=6. (D,E) Cells as in C but maintained in CHIR until DIV37 (n=3 biological replicates). One-way ANOVA analyses and post-hoc Kruskal–Wallis tests; asterisks above box plots indicate comparison against control, whereas asterisks above solid black bars indicate comparison between groups (n=15). *P<0.05, **P<0.01, ***P<0.001, ****P<0.0001. (F) Examples of nestin and βIII-tubulin imaging in different conditions as indicated by labels. (G) Schematic of long-term NPC cultures. (H) Cell expansion comparison between 'Control' and 'Niche' conditions in G. logΔcell: log2(most recent passage cell count number – previous passage cell count number). (I) ZBTB20-positive cell ratio. (J) DCX fibre length (process total length measured as in D,E). (I,J) Analyses were performed with a one-way ANOVA followed by a Kruskal–Wallis post-hoc test. ***P<0.001; n=3 biological replicates, 15 cell groups. In the box and whisker plots, the horizontal line indicates the median, the upper and lower edges of the boxes represent the bounds of the interquartile interval, and the whiskers represent the 99% confidence interval.

Development (2022) 149, dev200353. doi:10.1242/dev.200353

332 (α3,β3,γ2) and laminin 411 (α4,β1,γ1) (see Materials and Methods; Fig. 3B). We found that after 4 days *in vitro* in minimal medium without CHIR, these cells exhibited markedly different survival in membrane blebbing assays (Fig. S4A, Fig. 3C). We noticed a significant increase in membrane blebbing in cells plated on laminin 411 compared with laminin 511 (Fig. 3C). When we repeated these experiments with CHIR, these cells remained viable with all laminin isoforms, indicating that WNT signalling plays a key protective role in the hippocampal niche. We then lengthened the time of analysis to 9 days *in vitro* and assessed for NPC identity and neuronal differentiation markers nestin and βIII-tubulin, respectively (Fig. 3D-F, Fig. S4B). In comparison with laminin 511, we found that laminin 332 and laminin 411 significantly downregulated nestin^{+} fibres and msl induced a slight, albeit not significant, decrease (Fig. 3E). Laminin 121 supported nestin^{+} fibres almost to the same extent and was significantly increased by laminin 332 (Fig. 3D). However, laminin 121 also expressed the highest βIII-tubulin levels (Fig. 3E). Laminin 511 was thus deemed the most optimal laminin isoform for culturing NPC progenitor cells, given its membrane integrity retention and exclusivity in supporting NPCs.

hiPSC-derived hippocampal progenitor can be expanded *in vitro* for prolonged time

We used laminin 511 to continue to expand the niche of NPCs over the course of 230 days *in vitro*. Passaging cells every 14 days, we assayed two culture niches with different media to understand the minimal requirements necessary for prolonged expansion of NPCs. The niches always included laminin 511 and cells were either cultured in minimal medium (control, CHIR−) or medium with CHIR (Niche, CHIR+) (Fig. 3G). At every passage (~14 days), cells were counted and then re-seeded onto laminin 511 at equivalent surface densities (50,000 cells/cm^2). Using the cell count at each passage, we estimated the number of divisions occurring between passages of the two groups (Fig. 3H). We found that, without CHIR, cells exhausted their replicative ability over time and were not viable after DIV110. Constitutive CHIR instead seemed to provide the most stable growth until ~DIV180, whereafter approximate division number declined. To understand hippocampal stemness retention, we assayed both ZBTB20 and DCX expression (Fig. S5A and Fig. 3I,J). ZBTB20 expression remained stable under constitutive CHIR and laminin 511 despite the time of *in vitro* expansion (Fig. 3I). DCX was instead downregulated at DIV 240 (Fig. 3J). Our observations suggest the maintenance of a hippocampal identity in the CHIR-laminin 511 niche, which supports high neurogenic activity until 240 DIV.

We next investigated the differential contribution of laminin in supporting long-term culture (Fig. 4A). CHIR cells cultured from DIV 33 to DIV90 on laminin 511, in either progenitor maintenance conditions (PMC, 511+ CHIR) or spontaneous differentiation conditions (SDC, msl –CHIR), were compared with DIV33 CHIR cells for nestin and ZBTB20 expression (Fig. S5B, Fig. 4B).

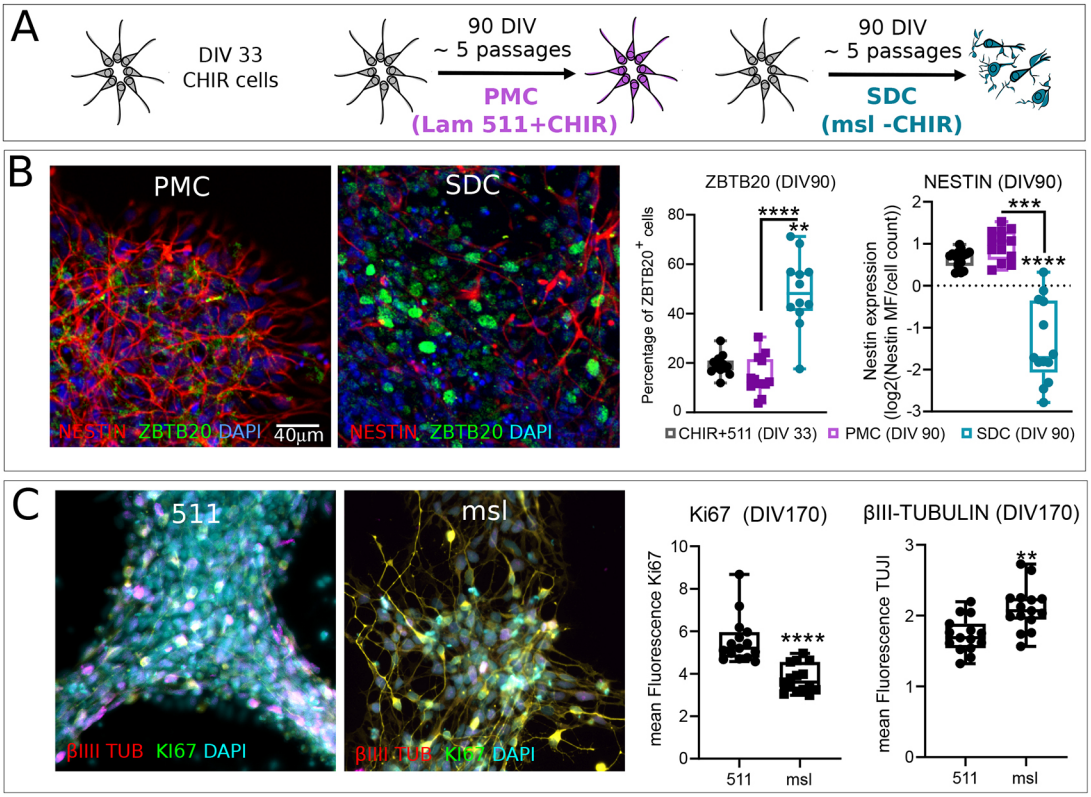

Fig. 4. Transition from laminin 511 to mouse laminin promotes differentiation of hippocampal NSCs. (A) Experimental overview. Three groups of cells: DIV33 naïve progenitors, NPCs grown in progenitor maintenance conditions (PMC, on 511 laminin and in 3 µM CHIR) until DIV90, and NPCs grown in spontaneous differentiation conditions (SDC, on msl and in minimal medium) until DIV90. (B) Cells imaged for nestin and ZBTB20. Groups were analysed with one-way ANOVA and post-hoc Kruskal–Wallis tests; asterisks above box plots indicate comparison against control. ***P*<0.01, ****P*<0.001, *****P*<0.0001; *n*=12. MF, mean fluorescence. (C) KI67 and βIII-tubulin imaging. DIV160 CHIR cells were plated on either laminin 511 or msl and kept in 3µM CHIR 99021 for 10 days, after which cultures were fixed and immunostained. Groups were analysed with Mann–Whitney nonparametric test; asterisks above box plots indicate comparison against 511. ***P*<0.01, *****P*<0.0001; *n*=15. In the box and whisker plots, the horizontal line indicates the median, the upper and lower edges of the boxes represent the bounds of the interquartile interval, and the whiskers represent the 99% confidence interval.

Development (2022) 149, dev200353. doi:10.1242/dev.200353

Whereas nestin expression is not significantly changed between DIV33 cells and the PMC condition, the SDC condition significantly downregulated nestin compared with both naïve and PMC cells (Fig. 4B). Furthermore, we observed a strong increase in ZBTB20^{+} cells in SDC cultures in comparison with both DIV33 cells and the PMC condition (Fig. 4B). Finally, we assayed whether DIV160 CHIR cells maintained differentiation competence. We cultured DIV 160 NPCs onto either laminin 511 or msl, sustaining both groups in CHIR for 10 days, and then assayed cultures for differentiating cells (Fig. S5C, Fig. 4C). We found that a single change in laminin at this culture age was enough to support differentiation despite CHIR presence in the media. In fact, Ki67 and βIII-tubulin appeared to be significantly down- and upregulated, respectively, after switching the cell substrate to msl (Fig. 4C). These results further substantiate that the laminin type is crucial for maintaining NPCs and indicate that, despite ∼6 months of *in vitro* expansion, DIV 160 cells were still capable of differentiating.

Laminin 511 supports NPC renewal by activating a specific set of genes

To better characterize the mechanisms of action of laminin 511, we directly compared its effect to the effect of msl in short-term experiments. We first compared the ratios of KI67-positive dividing NPCs and DCX-positive differentiating precursors in DIV28 CHIR cells seeded on the two different laminins and maintained 96 h in the presence of DAPT, to stimulate neuronal differentiation. The analysis was carried out 12 h after re-seeding the cells on either of the two different laminins (Fig. 5A). Laminin 511 supported lower DCX and higher KI67 cell ratios than msl (Fig. 5B,C). This was independent of the type of laminin re-seeding (see schematic in Fig. 5A). To investigate whether there was an effect due to differential adhesion of laminin 511 compared with mls, we analysed the difference between cells re-seeded onto different laminins. In this analysis, we labelled dividing NPCs with 5-ethynyl-2′-deoxyuridine (EdU) 24 h before re-seeding. The ratios of EDU-labelled cells were significantly higher when re-seeding cells from laminin 511 on laminin 511 compared with re-seeding on msl (Fig. 5D). Accordingly, the ratio of DCX-positive cells was significantly higher when re-seeding cells from msl on msl compared with re-seeding on laminin 511. These results indicate a higher cell adhesion capacity of laminin 511 compared with msl. Nonetheless, the differences due to 96 h culture in different laminins are much higher than the differences observed 12 h after re-seeding, indicating a stronger role for laminins in intracellular cell signalling rather than in mere cell adhesion.

To investigate the possible differences of signalling due to laminins, we analysed the global differential gene expression of DIV28 cells cultured on laminin 511, 48 h after re-seeding them onto laminin 511 or msl, with or without DAPT treatment. The PCA of their transcriptomes (Fig. 6A) indicates that the type of laminin they were cultured on accounted for most of the gene expression variance (first component=70.02%) whereas the variance due to DAPT treatment is under-represented (second component=

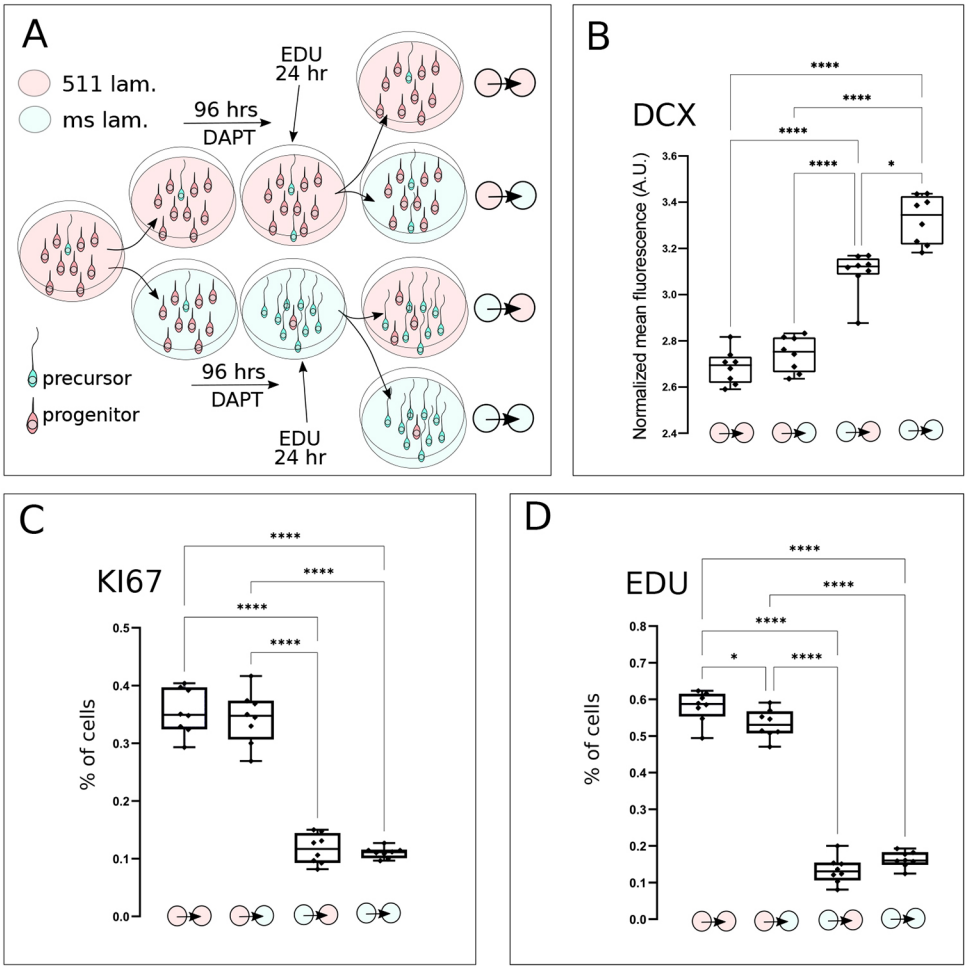

Fig. 5. Laminin 511 supports NPC expansion. (A) Outline of the experimental rationale showing the timing of drug addition and the type of laminin substrate, starting from DIV28 CHIR cells. (B-D) Quantification of different ratios of DCX-positive differentiating NPCs (B), KI67-positive dividing NPCs (C) and EDU-positive cells that underwent S-phase 1 day before re-seeding (D), as calculated by the analysis of cells imaged by ICD (DCX, HI-67) or azide fluorescence (EDU) 12 h after re-seeding. The arrows between coloured circles in B-D indicate the type of laminin transition as outlined in A. Three biological replicates per culture condition were analysed with two-way ANOVA analysis and post-hoc Tukey's multiple comparisons test. Asterisks above box plots indicate comparison among conditions. *n*=3 independent biological replicate each condition. **P*<0.05; *****P*<0.0001. In the box and whisker plots, the horizontal line indicates the median, the upper and lower edges of the boxes represent the bounds of the interquartile interval, and the whiskers represent the distribution of all data points.

Development (2022) 149, dev200353. doi:10.1242/dev.200353

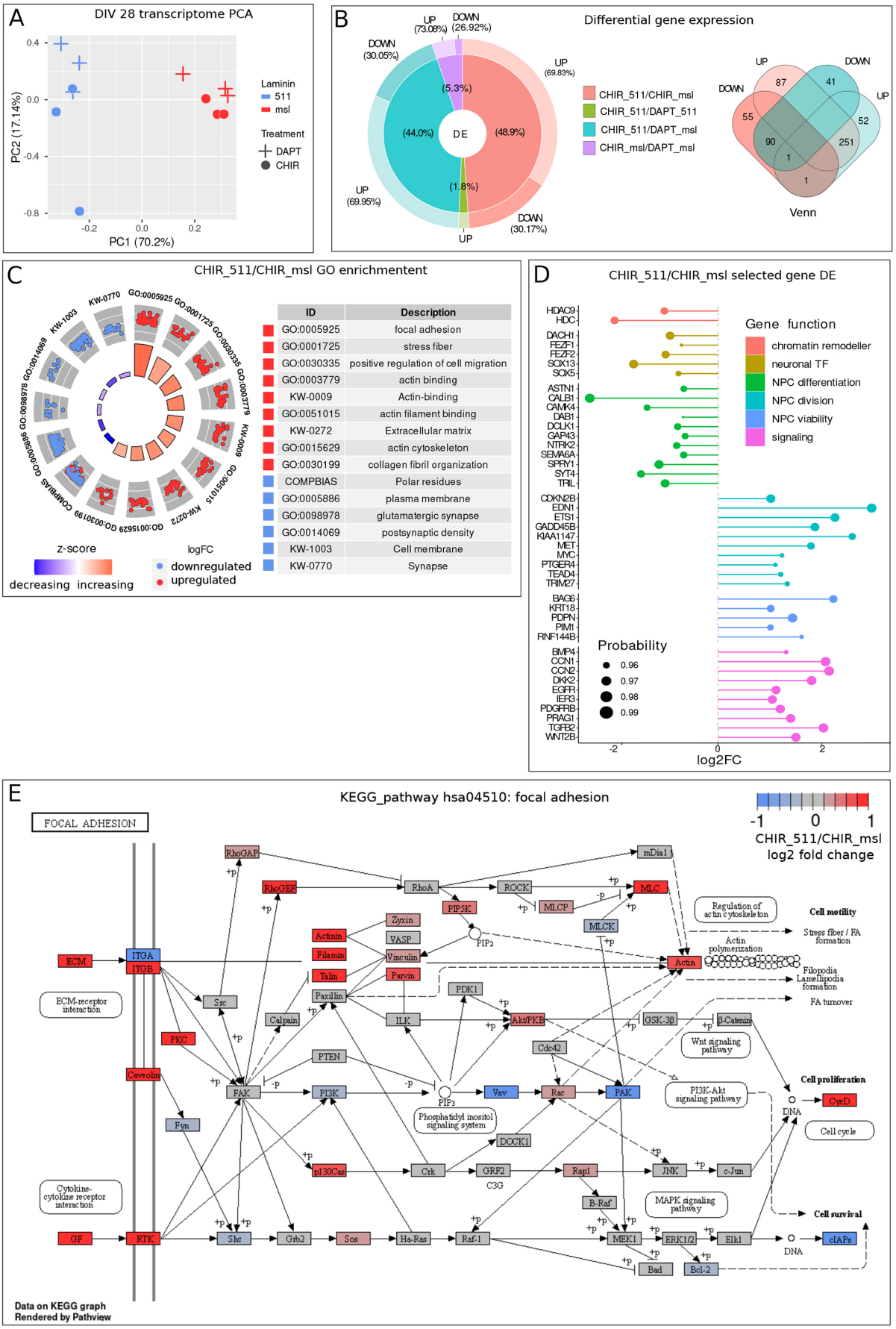

Fig. 6. See next page for legend.

Development (2022) 149, dev200353. doi:10.1242/dev.200353

Fig. 6. Laminin 511 supports NPC identity gene expression. (A-E) RNA-seq analysis of DIV28 CHIR cells after 48 h treatment in different combinations of laminin (laminin 511, msl) and medium (CHIR alone, CHIR; CHIR plus DAPT, DAPT). *n*=3 biological replicates per condition. (A) Transcriptome PCA. (B) The pie-donut diagram shows the proportions of DE genes between the conditions shown in legend (inner pie) and the contribution of up- and downregulation (UP and DOWN in the external donut). The Venn diagram shows the number of genes common to different experimental conditions. Significant differential expression was obtained by NOIseqBIO analysis (q>0.95). (C) GO term enrichment of DE genes between CHIR-511 and CHIR-msl conditions. The most enriched terms are reported, with FDR values ranging from $4.3\times e^{-17}$ to $2.17\times e^{-7}$ for upregulated genes and from $4.7\times e^{-4}$ to $1.5\times e^{-2}$ for downregulated genes. Z-scores were calculated by the GOplot package (R Cran). LogFC: log2(fold change). (D) Diagram reporting the log2(fold change) (log2FC) of selected DE genes between CHIR-511 and CHIR-msl conditions. DE genes were determined by NoiseqBIO (probability, q>0.95). (E) Diagram of focal adhesion gene pathway (KEGG-pathway hsa04510) enriched in the comparison between CHIR-511 and CHIR-msl conditions (FDR: $2.15\times e^{-9}$, *n*=24 genes, 7.14%). PathView package (Bioconductor) was used to generate the red-green heat colour code showing the levels of log2(fold change) gene expression. Coloured genes are differentially expressed between the two conditions.

17.14%). Consequently, the ratio of genes differentially expressed when shifting from laminin 511 to msl is much higher than the ratio when shifting from CHIR to CHIR+DAPT on the same laminin type (Fig. 6B, pie-donut chart). According to the known effect of Notch signalling inhibition by DAPT treatment, the Notch pathway genes *DLK1* and *HES1*, and the NPC marker NES, are differentially expressed between DAPT-treated and untreated cells, in the presence of msl. Moreover, the genes differentially expressed in these cells are significantly enriched in GO terms related to neuronal differentiation. Conversely, the genes differentially expressed between DAPT-treated and control cells, when cultured on laminin 511, are much fewer and show neither differential expression of markers of Notch signalling nor significant GO term enrichment, indicating that cells cultured on laminin 511 are less permissive than cells cultured on msl in responding to DAPT treatment (Fig. 6B, pie-donut chart). Finally, most of the genes upregulated and downregulated during the shift from laminin 511 to msl are shared between DAPT-treated and untreated cells, suggesting that the signalling induced by the laminin type prevails over Notch signalling inhibition (Fig. 6B, Venn diagram).

We focused on the nature of the genes differentially expressed depending on the laminin type (Table S3). The number of genes upregulated in cells cultured on laminin 511 is higher than the number of downregulated genes. This is reflected by the higher degree of GO term enrichment of upregulated genes (Fig. 6C). Genes highly expressed in cells cultured on laminin 511 are mainly enriched in terms related to the focal cell adhesion process whereas genes more expressed in msl-cultured cells belong to terms related to neuronal cell differentiation. To gain a deeper insight, we looked at the expression of selected genes among the most differentially expressed genes, which are known for their role in processes of NPC growth and differentiation. The analysis indicates that laminin 511 in general sustains NPC division, NPC viability and cell signalling, while msl supports chromatin remodelling, neuronal identity transcriptional control and NPC differentiation (Fig. 6D). Accordingly, most of the genes within the top enriched term, i.e. focal adhesion (KEGG_pathway, hsa04510), are downregulated during the shift from laminin 511 to msl (Fig. 6E). These include genes encoding extracellular and intracellular signalling molecules, and cyclin D, and might account for the dramatic effect of laminin 511 in supporting the expansion of the hippocampal neurogenic niche.

NPCs maintained in CHIR and laminin 511 for a long period retain the capacity to generate neurons

We assayed old CHIR cultures for their capacity to differentiate on msl, analysing NEUN and ZBTB20 expression (Fig. S6A, Fig. 7A). We found that, at DIV170, ZBTB20 was significantly upregulated in CHIR-DAPT-treated cells compared with DIV28 CHIR cells, although not to the same extent as in DIV50 CHIR-DAPT treatment, while NEUN was equally upregulated at both culture times. We concluded that older cultures maintain a hippocampal identity and the ability to undergo neuronal differentiation upon Notch inhibition. However, the significant difference in ZBTB20 expression suggested a change of identity between early and late CHIR cells. In fact, DIV50 and DIV170 CHIR cells show many DE genes (Fig. S6B). To delve deeper into this difference, we analysed the expression of a panel of genes specific for dentate gyrus (DG) or CA1-CA3 identity (Cembrowski et al., 2016). We observed that DIV50 CHIR-DAPT cells upregulated both DG and CA1-CA3 markers compared with DIV28 CHIR cells, indicating that these cultures can differentiate into all the different hippocampal mature neuronal cell types (Fig. 7B). Conversely, DIV170 CHIR-DAPT cells upregulated DG markers and downregulated CA1-CA3 markers compared with DIV28 cells (Fig. 7B). We speculate that late cultures behave as mature hippocampus, retaining the ability to produce DG granule cells but incapable of generating new CA1-3 neurons. Notably, this is the expected outcome of adult hippocampal neurogenesis from sub-granular zone (SGZ) progenitors (Gonçalves et al., 2016), although also parallels the expected maturation timing of CA epithelium and dentate epithelium in rodents (Altman and Bayer, 1990). Eventually, we analysed the nature of genes differentially expressed between DIV50 and DIV170 (843 upregulated and 1140 downregulated; Fig. S6B). The analysis of their GO enrichment highlights metabolic and chromatin reorganization processes, including upregulation of transcription factor activity, both RNAPII mediated and non-RNAPII mediated (Fig. S6C), suggesting that these cells might undergo an aging-like process *in vitro*.

Human hippocampal neurons integrate into *in vivo* hippocampus

To compare the capability of early and late CHIR cells to integrate *in vivo*, we labelled DIV30 and DIV180 CHIR cells by mGFP lentiviral transduction and transplanted them into adult mouse dentate gyrus (Fig. 8A,B). Cell survival and integration in the hippocampal circuitry were assessed after ∼3 months. We found neuronal processes of transplanted cells both in the DG around the transplant (Fig. 8B2) and in CA3 (Fig. 8B1). To assess synaptic contacts between grafted and host neurons, GFP^+ fibres in CA3 and DG were labelled with VGLUT1 and PSD-95 (Fig. 9A), and colocalization of GFP, VGLUT1 and PSD-95 was measured (Fig. 9B). We found no differences in terms of % area covered by synapses (Fig. 9C; two-way ANOVA, P=0.158) and synapse density (Fig. 9D; two-way ANOVA, P=0.435) between brain sections containing DIV30 and DIV180 grafted cells.

To compare area and density of DG-CA3 synapses made by grafted cells with those made by host mature hippocampal neurons, we injected Adeno-associated virus (AAV) carrying GFP expression under the synapsin promoter in the DG of adult wild-type mice. Quantification of GFP, VGLUT1 and PSD-95 colocalization showed no differences in terms of area covered by GFP^+ synapses between grafted and AAV infected mice (Fig. 9E; two-way ANOVA, P=0.408). However, we found significant statistical differences in terms of synapses density

Development (2022) 149, dev200353. doi:10.1242/dev.200353

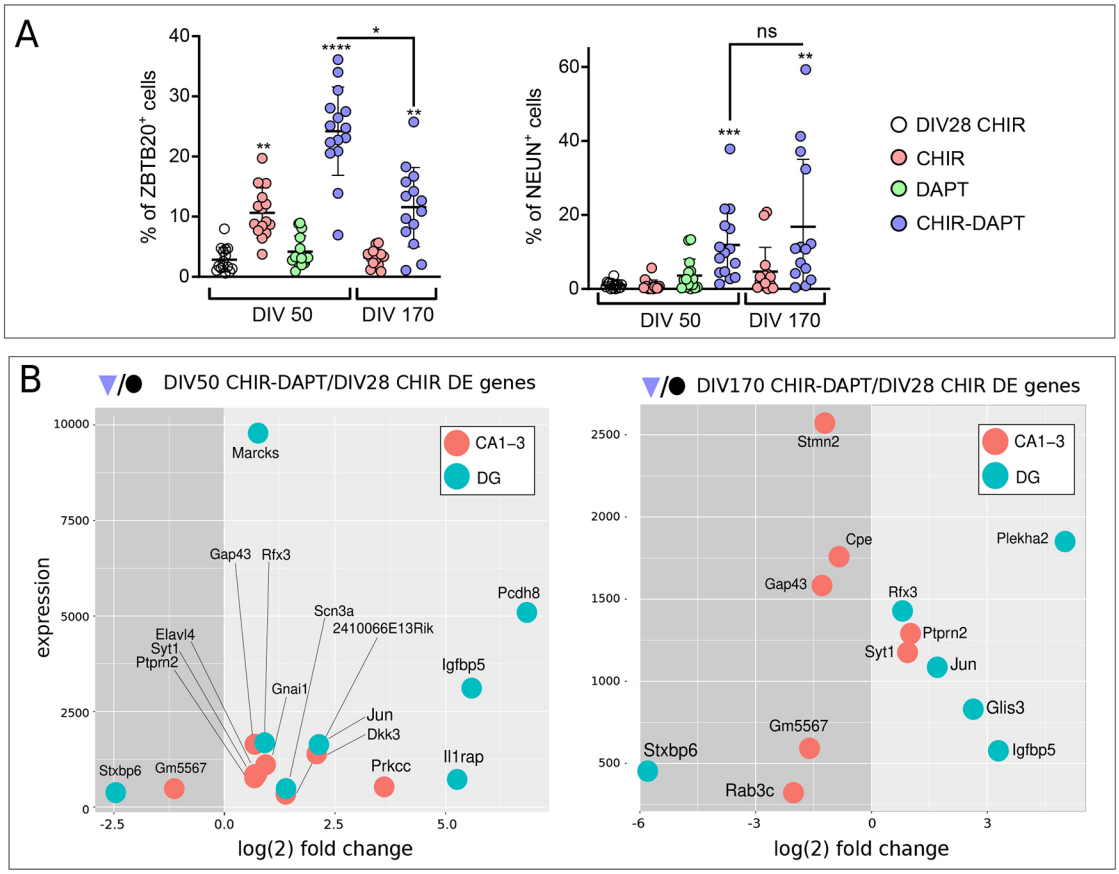

Fig. 7. Early and late CHIR cells maintain neurogenic capacity. (A,B) DIV40 and DIV160 CHIR cells were plated on msl and cultured until DIV50 and DIV170, respectively, in minimal media (Control), or treated at DIV46 and DIV166 for 2 days with CHIR, DAPT or CHIR-DAPT. Inhibitors were removed after 2 days, and cells were maintained in minimal media for 2 more days before analysis (DIV50 and DIV170); *n*=3 biological replicates for each condition. (A) Percentage of cells positive for ZBTB20 and NeuN at the different times and culture conditions, as indicated by labels. Statistical analyses were performed by one-way ANOVA, post-hoc Kruskal–Wallis test; asterisks above plotted values indicate comparison against control, whereas asterisks above solid black bars indicate comparison between groups; error bar represent 99% confidence interval. **P*<0.05, ***P*<0.01, ****P*<0.001, *****P*<0.0001. (B) M-D plots of RNA-seq analysis of markers of DG or CA1-3 layers in cells as in A, differentially expressed between the culture conditions indicated in labels (NOIseq analysis, q>0.8).

between endogenous and grafted fibres (Fig. 9F; two-way ANOVA, P=0.011). In particular, post-hoc comparisons revealed significant differences in the CA3 region (Tukey's test, P=0.033) and a tendency towards a difference in the DG region (Tukey test's, P=0.073). Species-intrinsic differences and time of maturation might have accounted for these observations (see Discussion). Nonetheless, our results confirm that the differentiation and maturation capabilities are retained by hiPSC-derived hippocampal progenitors maintained in the CHIR-laminin 511 niche. Moreover, the area covered by synapses was similar in GFP$^+$ fibres belonging to grafted and endogenous DG neurons, despite the density being higher in host cells.

DISCUSSION

WNT signalling induces a hippocampal cell identity in a narrow time window of hiPSC neuralization

The hippocampus is a fundamental brain structure hosting one of the two adult brain neurogenic niches. Although extensively studied, both extrinsic and intrinsic cues orchestrating cell identity specification, neurogenic activity, layer specification and aging are substantially unsettled in humans. Herein, we established a protocol to simulate hippocampal fating and extended propagation of hippocampus-like neural stem cell populations. WNT signalling is a necessary pathway in hippocampal fating (Grove and Tole, 1999) but also in regulating adult neurogenesis (Arredondo et al., 2020; Ni et al., 2021). CHIR99021 (CHIR), which induces WNT signalling via indirect activation of the β-catenin pathway (Naujok et al., 2014), has previously been used in *in vitro* hippocampal models of hESC and mESC differentiation (Sakaguchi et al., 2015; Terrigno et al., 2018). Here, we demonstrate that CHIR upregulates hippocampal developmental markers to differentiate hiPSCs with an identity similar to hippocampal neuroepithelial cells. Starting from hiPSCs committed to dorsal telencephalic identity (Martins et al., 2021; Shi et al., 2012b), the addition of CHIR to minimal culture medium for 12 days in a specific time window of differentiation is sufficient to generate NPC populations with hippocampal identity. These populations significantly upregulated PROX1, DCX, BCL11B and ZBTB20, which are key markers of embryonic hippocampal cells (Iwano et al., 2012; Knoth et al., 2010; Nielsen et al., 2014; Simon et al., 2012). Moreover, the global gene expression profile of these cells is similar to the profile of human hippocampal embryonic cells, as demonstrated by transcriptome-wide clustering analysis.

The analysis of hippocampal scRNA-Seq datasets confirms that ZBTB20 is one of the most robust markers of hippocampal identity. Using ZBTB20 as reporter, we could assay the different effects of

Development (2022) 149, dev200353. doi:10.1242/dev.200353

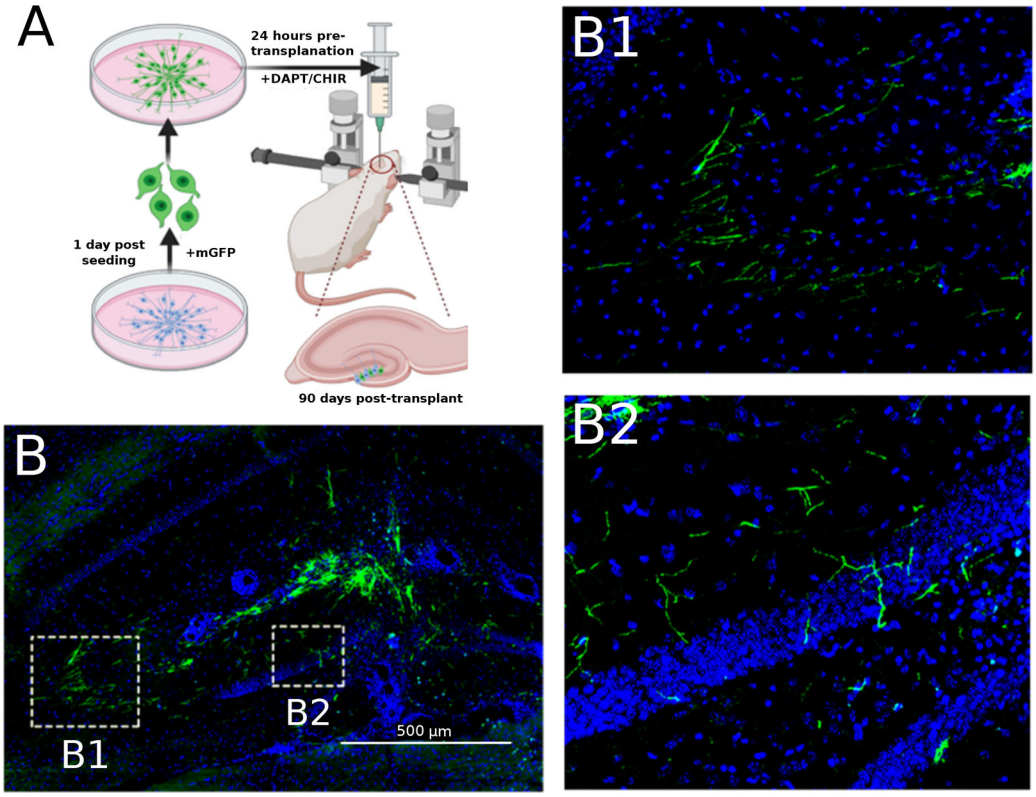

Fig. 8. *In vivo* transplantation of CHIR cells into mouse hippocampal DG. (A) Experimental scheme: after 30 or 180 days *in vitro*, CHIR cells were infected with a GFP-expressing lentiviral vector, treated 24 h with DAPT and transplanted in the DG of adult wild-type mice. (B) Micrograph of the hippocampal grafted cells (GFP+) in the host dentate gyrus (Hoechst). Magnifications of the outlined areas show GFP$^+$ fibres elongated in the peritransplant DG area (B2) and in CA3 (B1).

Notch and WNT signalling in establishing a hippocampal identity in neuralized hiPSCs and found that WNT is necessary for hippocampal specification independently of the state of Notch signalling. This conclusion is further supported by the analysis of GO term enrichment of the genes differentially expressed upon WNT and Notch activation.

Laminin 511 is an essential signalling component of the hippocampal neurogenetic niche

Because the hippocampal niche sustains continuous neurogenesis throughout embryonic and post-natal life, we sought to recreate a model of SGC niche *in vitro*, to further understand the signalling machinery involved. We focused on the ECM component of the niche because it is the least described. Laminins are one of the major protein groups in the extracellular matrix (ECM). They are heterotrimers of five α-, three β- and three γ-subunits with different expression patterns in distinct developing and adult brain regions, and they interact with integrins and non-integrin receptors, such as dystroglycan, mediating cell adhesion and intracellular signalling (Nirwane and Yao, 2019). The mechanisms of laminin signalling have not been completely elucidated. In hiPSCs, laminin 511 binds to α3β1-, α6β1- and α6β4-integrin, inducing activation of the PI3K/AKT-dependent and Ras/MAPK-dependent signalling pathways. Moreover, the interactions of laminin-511 and α6β1-integrin with E-cadherin inhibit apoptosis mediated by the Rho kinase (ROCK) signalling pathway (Nakashima and Omasa, 2016). Most of the studies on the role of laminins and integrins on neural progenitor proliferation and differentiation have been performed in culture or non-mammal models. Laminin stimulates expansion and differentiation of hESC-derived neural progenitors via interaction with α6- or β1-integrin subunits (Ma et al., 2008). Loss of β1-integrin generates smaller neurospheres through MAPK signalling (Campos et al., 2004). Interestingly, overexpression of constitutively active β1-integrin in the embryonic chick mesencephalon enhances the number of mitotic progenitors, analogous to sub-apical progenitors in mouse, through a non-cell autonomous mechanism that is mediated by the upregulation of Wnt7a (Long et al., 2016).

Previous *in vivo* reports have indicated the necessity of α5 laminin subunit in the cortical SVZ niche to propagate neural stem cell populations (Nascimento et al., 2018). We thus compared laminin α5β1γ1 (laminin 511) against other laminin isoforms associated with either neuronal cell survival, such as α1β2γ1 (laminin 121) (Sasaki et al., 2010), laminin isoforms of peripheral epithelial and endothelial niches (α3-β3-β2 and α4-β1-β1; laminin 332 and 411) (Hall et al., 2022; Kiritsi et al., 2013) or a purified mouse laminin isoform (α1-β1-β1; msl) (Horejs et al., 2014). Indeed, we confirmed that laminin 511 exclusively promoted NPC survival and maintenance in comparison with the other four substrates. We then cultured hippocampal NPC populations from DIV 28 onwards, using laminin 511 as the substrate, and found that these populations could be expanded over 200 days *in vitro* with little to no deviation from a progenitor-like condition, as indicated by DCX downregulation. These cells were still able to differentiate if transferred from laminin 511 to msl. The observation that laminin 511 supports continuous expansion of the hippocampal niche sheds light on a new aspect of the hippocampal neurogenic molecular machinery to be addressed in detail in future studies. Here, we report

Development (2022) 149, dev200353. doi:10.1242/dev.200353

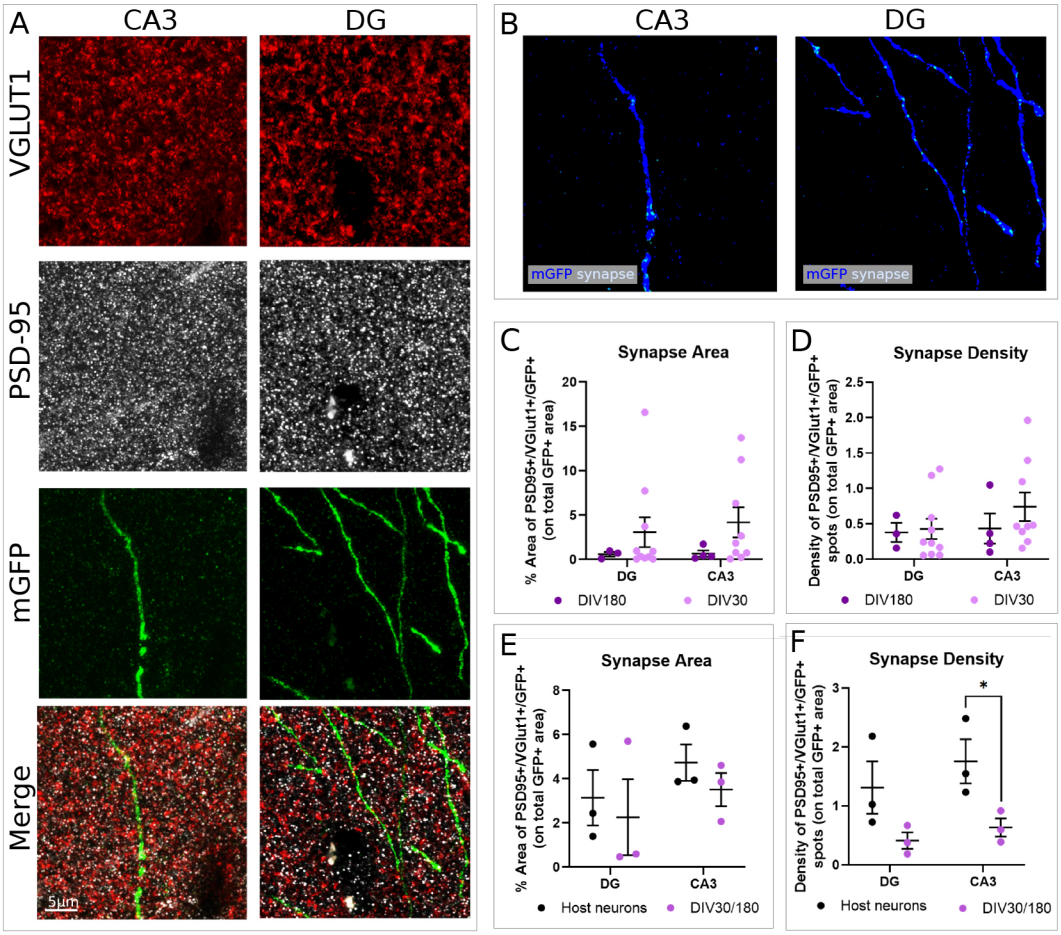

Fig. 9. Quantification of GFP$^+$ synapses in DIV30, DIV180 and host neurons. (A) Immunostaining of VGLUT1, mGFP and PSD-95 in fibres of transplanted and host neurons of CA3 and DG. (B) Synapses of transplanted neurons were imaged considering pixels positive for VGLUT1, PSD-95 and mGFP (light-blue signal). Positive pixels were then superimposed to mGFP (dark-blue signal). (C,D) Synapse quantification was performed considering positive pixels as in B. Synapses were measured in terms of density and percentage of GFP$^+$ area covered by synapses. Comparisons between sections acquired from brains injected with DIV30 and DIV180 CHIR cells showed no statistical differences in terms of percentage of area covered by synapses (two-way ANOVA, P=0.158) (C) and synapses density (two-way ANOVA, P=0.435) (D). DG: n=3 sections (DIV180), n=10 sections (DIV30). CA3: n=4 sections (DIV180), n=9 sections (DIV30). (E) Additionally, the percentage of area covered by synapses was similar between grafted and endogenous hippocampal neurons, which were labelled with a GFP-expressing AAV injected in the DG of wild-type control animals (two-way ANOVA, P=0.408). (F) Nonetheless, synapse density of grafted neurons resulted lower than endogenous neurons in CA3 region (two-way ANOVA, P=0.033) but not in the DG region (two-way ANOVA, P=0.077) (n=3 mice per group). Data are mean±s.e.m.

a preliminary analysis of the mechanisms by which laminin 511 supports the expansion of NPCs in culture. Our analysis of the short-term effects after cell re-seeding on laminin 511 or msl indicates that laminin 511 mostly acts as a key signalling factor influencing gene expression. The results of RNA-seq indicate a dramatic effect of laminin 511 directly or indirectly sustaining the expression of genes related to NPC identity, expansion and viability through the activation of key members of the focal adhesion pathway. We speculate that msl promotes NPC differentiation because of its much lower efficiency than laminin 511 in supporting NPC stemness and proliferation by focal adhesion gene activation. Notably, the extent of gene expression control by laminin 511 is dramatically higher than the control level exerted by Notch signalling. Moreover, the intracellular signalling activated by laminin 511 is sufficient to bypass the Notch signalling, as suggested by the inability of cells cultured on laminin 511 to activate neuronal markers upon DAPT treatment. Our observations suggest a crucial role for laminin components in the hippocampal neurogenic niche and open new routes to the comprehension of the contribution of ECM to hippocampal cell stemness. These include detailed studies of laminin receptor expression in hippocampal progenitors, and their functional role in laminin-directed intracellular signalling.

WNT-laminin 511 niche sustains hippocampal NPC expansion and maturation *in vitro*

The differences of expression of markers of DG and CA1-CA3 layer identity observed between early and late cultures induced to differentiate by msl and DAPT suggest that long-term expansion of hippocampal progenitors within the WNT-laminin 511 niche induced changes in NPC competence. We speculate that our culture conditions somehow prompted NPCs to mature *in vitro* in a way that recapitulates prenatal *in vivo* development: in fact, late cultures keep expressing granule DG markers but downregulate CA1-CA3 markers, as it occurs at the end of pre-natal neurogenesis (Altman and Bayer, 1990; Gonçalves et al., 2016).

The hippocampus is a highly selective brain region with respect to cell survivability and integration, as previous heterologous cell-region transplantations have demonstrated (Quattrocolo et al., 2017;

Development (2022) 149, dev200353. doi:10.1242/dev.200353

Terrigno et al., 2018). Although successful xenografting of hiPSC-derived NPCs into the DG of adult host mice cannot rule out the possibility that the transplanted cells are not bona fide human hippocampal neurons, it indicates that their long-term expansion *in vitro* has not altered their capacity to terminally differentiate and integrate into a host hippocampal tissue. Notably, the analysis of the molecular synaptic markers in the xenografts supports the idea that transplanted and resident neurons generate synapses at a similar extent, because the area of GFP^+ synapses is not significantly different between grafted and AAV-infected mice. However, the synaptic density of the grafted cells is lower than the synaptic density of resident cells. We speculate that this result might be due to intrinsic structural differences of the synapses in and/or between the two species, and we suggest that human-human and human-mouse cell synapses within xenografts might occupy a larger volume compared with mouse-mouse cells synapses.

Finally, our results contribute to understanding the key changes of gene expression occurring during human hippocampus development and indicate a previously unreported role for laminin 511 in supporting the *in vitro* expansion of a hippocampal neurogenic niche. The implications of this study may open new avenues for studying cell type-dependent neurogenesis, synaptic transmission in the hippocampus and future cell-based therapies.

MATERIALS AND METHODS

hiPSC culture and differentiation

For both cell expansion and differentiation, hiPSCs (ATCC, catalogue DYS0100) were seeded onto Geltrex LDEV-Free Reduced Growth Factor Basement Membrane Matrix (Thermo Fisher Scientific, A1413202) in Essential 8 Medium (Thermo Fisher Scientific, A1517001) containing Essential 8 Medium Supplement (Thermo Fisher Scientific, A1517-01), 100 U/ml penicillin-streptomycin and 2 µM Y-27632 (Cell Guidance Systems, SM02-5). 24 h later, E8 containing Y-27632 was aspirated and fresh E8 medium without Y-27632 was added. E8 medium was changed daily for another 2 days. For neural differentiation, cells were incubated in WNT/BMP/TGF-β triple inhibition (WiBiTi) medium [DMEM/F-12 (Thermo Fisher Scientific, 11320033) containing 2 mM glutamine, 1 mM sodium pyruvate, 100 U/ml penicillin-streptomycin, 1 mM non-essential amino acids, 0.05 mM β-mercaptoethanol, 10 µM 53AH (WNT inhibitor, Cellagen Technology, C5324-2 s), 10 µM LDN193189 hydrochloride (BMP inhibitor, Sigma-Aldrich, SML0559), 1 µM RepSox (Sigma-Aldrich, R0158-5MG, TGFβ inhibitor), N-2 Supplement 100× (Thermo Fisher Scientific, 17502001) and B-27 Supplement minus Vitamin A 50× (Thermo Fisher Scientific, 12587010)]. The day of shift from Essential 8 Medium to WiBiTi medium is DIV 0. WiBiTi medium was changed daily until DIV 10 where cells were passaged and reseeded in N2B27 medium containing Y-27632 at a density of 200,000 cells/cm^2 on culture dish pre-coated with Poly-ornithine (P3655 Sigma-Aldrich; 20 µg/ml in sterile water, 24 h coating at 37°C) and laminin iMatrix-511silk E8 (human laminin 511, Amsbio, AMS.892 021, 24 h coating at 37°C). Less than 24 h later, N2B27 containing Y-27632 was aspirated and fresh WiBiTi medium without Y-27632 was added. Cells were maintained in WiBiTi medium for another 4 days until DIV 15, where the medium was changed to N2B27.

To induce hippocampal identity, the following day (DIV 16) cells were then cultured for an additional 6 days (DIV 21) in CH27 medium (N2B27 medium supplemented with 3 µM CHIR99021; Sigma-Aldrich, SML1046-5MG). At DIV 21, cells reached confluence and required another passage in CH27 medium supplemented with Y-27632 and onto poly-ornithine/laminin 511-coated plastic at a density of 200,000 cells/cm^2. Less than 24 h later, CH27 containing Y-27632 was aspirated and fresh CH27 medium without Y-27632 was added. Medium was changed daily with fresh CH27 until DIV 28 wherein cells, named CHIR cells, were passaged for longitudinally maintaining the CHIR NSC niche or used for differentiation experiments.

When different laminins were used, Poly-ornithine was pre-coated for 24 h at 37°C, followed by coating with 2.5 µg/ml of specific laminin in PBS for 24 h at 37°C. The following laminins were used: natural mouse laminin (msl, 111, 23017015, Thermo Fisher Scientific); laminin 121, Biolaminin 121 LN (LN121); laminin 332, Biolaminin 332 LN (LN332); and laminin 441, Biolaminin 441 LN (LN441).

Maintaining hippocampal NSC niche

Starting from DIV 28, CHIR NPCs were passaged and reseeded in N2B27 medium containing Y-27632 at a density of 100,000 cells/cm^2 on poly-ornithine/511 human laminin-coated plastic. Less than 24 h later, CH27 containing Y-27632 was aspirated and fresh CH27 medium without Y-27632 was added. CH27 medium was changed daily for 2 weeks from the reseeding date (DIV 42) whereupon cells were passaged again in an identical manner until DIV 200. Approximate cell counts were recorded per split and sample pellets for qRT-PCR were also collected.

hiPSC-derived NPC differentiation

NPCs, regardless of age, do not differentiate on laminin 511 and attempted differentiation resulted in cell detachment and death. When ready to differentiate, either endogenously or by Notch inhibitor (DAPT), CHIR cells were seeded onto plates coated with poly-ornithine msl. For immunocytodetection, cells were seeded onto Eppendorf biofilm-bottom plates (Eppenforf, EP0030722019) or on a layer of mESC-derived hippocampus neurons, derived using the protocol of Terrigno et al. (2018). After passaging/thawing, cell suspensions were centrifuged at 200 ***g*** for 4 min and the cell pellet resuspended in CH27 supplemented with Y-27632. Less than 24 h later, CH27 containing Y-27632 was aspirated and fresh CH27 medium without Y-27632 was added. Medium was changed daily with fresh CH27 until cells reached 90% confluence (after ∼10 days), whereupon CH27 medium was changed to medium containing DMEM/F-12, 2 mM glutamine, 1 mM sodium pyruvate, 100 U/ml penicillin-streptomycin, 0.05 mM β-mercaptoethanol, N-2 supplement (100×), B-27 supplement (50×) (with Vitamin A, Thermo Fisher Scientific, 125870-01), 20 ng/ml recombinant human BDNF (NBP2-52006, Novus Biologicals) and 0.5 mM ascorbate (A92902, Sigma-Aldrich). Experimental differentiation medium included 3 µM CHIR99021 (CHIR) or 12.5 µM DAPT (Sigma-Aldrich D5942), or both.

Cell culture imaging

Cells were fixed for 10 min in 2% paraformaldehyde, permeabilized and blocked in 3% foetal calf serum, 3% bovine serum albumin and 0.2% Triton in PBS at room temperature for 1 h. Primary antibodies were incubated at 4°C in PBS, 3% FCS and 3% BSA ranging from overnight (for cytoskeletal/membrane proteins) up to 72 h (for nuclear antigens). Secondary antibody was incubated under the same conditions for ∼1.5 h at room temperature. After PBS washes and nuclear staining with Hoechst, cells were mounted in Aqua/Poly-mount (Polysciences, 18606-100) and stored at 4°C before imaging. Images were produced on a Leica SP2 confocal microscope or Zeiss confocal microscope by acquiring *z*-stack images 10-15 optical slices thick, each slice ∼1 µm.

Previously released ImageJ macros (https://imagej.net/scripting/batch) were employed to batch analyse stack fluorescence parameters, including fluorescent signal magnitude and density, fluorescent cell count, total approximate fibre length, conversion of full experiment stacks to individual component TIFFs and conversion of full experiment stacks to the compressed single channel representative PNGs. The only parameters changed were cell area, which is dependent on the objective, and binary threshold, which is dependent on the relative signal-to-noise ratio of fluorescence marker in an independent experiment.

RNA extraction

All *in vitro* samples used for transcriptomic assays were harvested by 5′, 37°C trypsinization. Detached cells were homogeneously suspended in solution, collected in microcentrifuge tubes and pelleted at 200 ***g*** for 5 min. After centrifugation, the supernatant was aspirated and the cell pellet was disrupted and processed using NucleoSpin RNA kit (Machery-Nagel, 740955.250). RNA concentration was measured using a NanoDrop Lite Spectrophotometer (Thermo Fisher Scientific, ND-LITE).

Development (2022) 149, dev200353. doi:10.1242/dev.200353

qRT-PCR analysis of human and mouse cells

RNA extracted from *in vitro* samples were processed using Reverse Transcriptase Core Kit 300 (Eurogentec, RT-RTCK-03). Approximately 200 ng of RNA was reverse transcribed into cDNA for qRT-PCR analysis. SensiFAST SYBR mix (12 µl, BioLine, BIO-98020) and cDNA (8 µl) were combined in 4titude PCR quality tubes and quantified using Qiagen 72-Well Rotorgene as previously described (Terrigno et al., 2018).

RNA-seq

RNA-seq libraries were prepared with either the SMART-Seq HT PLUS Kit (Takara; used for CHIR differentiation experiments) or the Stranded Total RNA Prep with Ribo-Zero Plus Kit (Illumina; used for laminin comparison) following manufacturer's instructions. Pooled reads were sequenced on a NovaSeq machine (Illumina), obtaining between 20 and 50 M reads per sample.

Transcripts were pseudoaligned using Salmon (Patro et al., 2017) in mapping-based mode (with its default '–validateMappings' flag). A decoy-aware version of the Ensembl mouse transcriptome (mm10; http://refgenomes.databio.org/) was used as a reference. RNA-seq analysis was carried out using the R package NOISeq. Raw counts were normalized with the Trimmed Mean of M values (TMM) method. Low-count filtering was performed with the CPM method, using cpm=1 as threshold. PCA exploration was carried out to confirm that the experimental samples were clustered according to the experimental design (see Fig. 2A, Fig. 6A). Differential expression was calculated by the NOISeq or NOISeqBIO method and a significance threshold of q=0.8 or q=0.95 was applied, respectively. RNA-seq data from Allen Brain Atlas (Colantuoni et al., 2011) were compared with hiPSCs data upon scaling of both datasets to percent and by applying the hclust (distance) and prcomp R Cranpackages. Raw genomic data and expression counts have been deposited in the Gene Expression Omnibus database under accession number GSE199355.

COTAN analysis of scRNA seq dataset

Co-expression table analysis (COTAN) (Galfrè et al., 2021) was used to find an approximation of the probability of zero read counts for a gene in a cell, testing the null hypothesis of independent expression for gene pairs, by counting zero/non-zero unique molecular identifier (UMI) counts in single cells. Expected values for contingency table analysis were obtained using UMI detection efficiency (UDE), average expression of genes was estimated using linear method and gene dispersion was estimated by fitting the observed number of cells with zero UMI count. COTAN provided both an approximate *P*-value for the test of independence and a signed co-expression index (COEX), which measures the direction and intensity of the deviation from the independence hypothesis. Plots were generated with ggplot2 in R environment. The following R Cran packages were employed: matrixStats, ggfortify, dplyr, rray, propagate, data.table, ggsci, gmodels, parallel, tibble and ggrepel.

In vivo assay of neural precursors survival and integration

All experiments were carried out in accordance with the EU Council Directive 2010/63/EU on the protection of animals used for scientific purposes, and were approved by the Italian Ministry of Health (authorization number 739/2017-PR). Mice were housed in standard conditions with water and food *ad libitum* and a 12 h dark/light cycle. A total of 13 C57BL6/J mice were used, five were grafted with DIV30 cells, five with DIV180 cells and three mice were injected with AAV-GFP as controls. Mice injected with cells were treated daily with subcutaneous injections of cyclosporine A (Sandimmun, 10 mg/kg) from the day before the injection to 3 weeks after and then cyclosporine A was delivered in the drinking water (Sporimune, 0.21 mg/ml) and refreshed every 3 days. Of the 10 cell-injected mice, one DIV30 died post-surgery, two DIV30 and two DIV180 showed no successful grafts in the DG, three DIV180 showed a small graft with few fibres (not reaching the CA3). One DIV180 and two DIV30 mice showed a considerable amount of fibres in both CA3 and DG; thus, only these animals were considered in the synapse quantification.

On the day of the transplantation, cells were detached from culture substrate by removing culture medium, washing with 1× Versene (Thermo Fisher Scientific, A4239101) and incubating with minimal volume of Accutase (A6964, Sigma-Aldrich) for 25 min at 37°C. At the end of the incubation, Accutase was diluted in fresh 1× PBS in a volumetric ratio of 1 Accutase:10 PBS. Cell suspension was centrifuged at 1700 ***g*** for 4 min at room temperature and resuspended in a volume of foetal bovine serum sufficient to concentrate cells at 100,000 cells/µl. Cells were maintained at 4°C until they were injected. Mice were anesthetized using a cocktail of hypnorm (0.38 mg/kg) and hypnovel (12 mg/kg), and placed in a stereotaxic frame. The scalp was opened and the head bone sutures exposed for reference. Cells (100,000 cells/µl) were injected in the dentate gyrus through three injection sites (2, 1.7 and 2.3 mm A; 1.5 mm ML; 1.7 mm DV from Bregma), delivering 0.5 µl for each site, using a Hamilton syringe connected to a motorized pump (Legato130). Cells were gently resuspended, loaded (2 µl, 2 µl/min) in the syringe and infused (0.3 µl/min) in the three brain sites. After the injection, the syringe was left in place for 2 min, before being removed, emptied and washed with saline and cell medium. The skin was sutured and mice were placed on a heating pad and allowed to waken.

Imaging of human cells in mouse hippocampal sections

At 3 months post-transplantation, mice were transcardially perfused with PFA 4%. Brains were collected and sliced using a freezing microtome, to obtain 30 µm coronal sections. After 1 h in blocking solution, free-floating sections were incubated overnight with primary antibodies anti-GFP (goat, Abcam), anti-PSD95 (rabbit, Abcam) and anti-VGLUT1 (guinea pig, SYSY). After rinsing, secondary antibodies (Alexa488 anti-goat, CY5 anti-rabbit and RRX anti-guinea pig, Jackson) were used for immunostaining. Cell nuclei were stained using Hoechst. For antibody details, see Table S4.

Images for synapse quantification were acquired with a Plan Apochromat 63×/1.4 NA oil DIC M27 objective lens with a Axio Observer 7 microscope on a LSM 900 Airyscan2 confocal (Carl Zeiss) equipped with 488, 561 and 640 lasers. The total thickness of the *z* stacks was 2-3 µm and the distance between adjacent focal planes was set at a constant value of 0.15 µm intervals.

For each animal (n=6), one field in CA3 and one in the DG region were acquired in at least three sections with visible GFP+ fibres. Stacks were opened in ImageJ2/Fiji (https://imagej.net/software/fiji/), using a custom-made macro, each channel was thresholded and only particles with an over threshold signal in all three channels were considered and counted as synapses. Using a Matlab custom-made script, for each plane, total area and number of selected synapses were expressed as percentage of total GFP^+ threshold area, and then averaged among focal planes of each stack.

Acknowledgements

We thank M. A. Calvello and V. Liverani for technical support; L. Conti for induced pluripotent stem cell neural differentiation methods advice; and Dr D. Vozzi and the IIT Neurogenomics facility for transcriptomic library sequencing. We are immensely grateful to M.C. for his contribution as a scientist and man.

Competing interests

The authors declare no competing or financial interests.

Author contributions

Conceptualization: M.C., L.P., C.A., F.C.; Methodology: K.D., F.T., E.N., A.C., V.M., F.B., L.P., C.A.; Software: S. Galfrè; Formal analysis: K.D., S. Gustincich, M.C., L.P., C.A.; Investigation: K.D., E.N., A.C., V.M., A.M.F.; Resources: S. Gustincich, M.C., L.P., C.A.; Data curation: K.D.; Writing - original draft: K.D., L.P.; Writing - review & editing: C.A., L.P., F.C.; Supervision: F.C.; Project administration: F.C.

Funding

This work was supported by the European Commission FP7 PAIN-CAGE project (603191) and by the H2020 LEIT Information and Communication Technologies 2016 MADIA project (732678).

Data availability

Raw genomic data and expression counts have been deposited in GEO under accession number GSE199355.

References

Abellán, A., Desfilis, E. and Medina, L. (2014). Combinatorial expression of Lef1, Lhx2, Lhx5, Lhx9, Lmo3, Lmo4, and Prox1 helps to identify comparable subdivisions in the developing hippocampal formation of mouse and chicken. *Front. Neuroanat.* **8**, 59. doi:10.3389/fnana.2014.00059

Åberg, M. A. I., Åberg, N. D., Hedbäcker, H., Oscarsson, J. and Eriksson, P. S. (2000). Peripheral infusion of IGF-I selectively induces neurogenesis in the adult rat hippocampus. *J. Neurosci.* **20**, 2896-2903. doi:10.1523/JNEUROSCI.20-08-02896.2000

Ables, J. L., Decarolis, N. A., Johnson, M. A., Rivera, P. D., Gao, Z., Cooper, D. C., Radtke, F., Hsieh, J. and Eisch, A. J. (2010). Notch1 is required for maintenance of the reservoir of adult hippocampal stem cells. *J. Neurosci.* **30**, 10484-10492. doi:10.1523/JNEUROSCI.4721-09.2010

Altman, J. and Bayer, S. A. (1990). Migration and distribution of two populations of hippocampal granule cell precursors during the perinatal and postnatal periods. *J. Comp. Neurol.* **301**, 365-381. doi:10.1002/cne.903010304

Altman, J. and Das, G. D. (1965). Autoradiographic and histological evidence of postnatal hippocampal neurogenesis in rats. *J. Comp. Neurol.* **124**, 319-335. doi:10.1002/cne.901240303

Arredondo, S. B., Guerrero, F. G., Herrera-Soto, A., Jensen-Flores, J., Bustamante, D. B., Oñate-Ponce, A., Henny, P., Varas-Godoy, M., Inestrosa, N. C. and Varela-Nallar, L. (2020). Wnt5a promotes differentiation and development of adult-born neurons in the hippocampus by noncanonical Wnt signaling. *Stem Cells* **38**, 422-436. doi:10.1002/stem.3121

Asrican, B., Wooten, J., Li, Y.-D., Quintanilla, L., Zhang, F., Wander, C., Bao, H., Yeh, C.-Y., Luo, Y.-J., Olsen, R. et al. (2020). Neuropeptides modulate local astrocytes to regulate adult hippocampal neural stem cells. *Neuron* **108**, 349-366.e6. doi:10.1016/j.neuron.2020.07.039

Berdugo-Vega, G., Arias-Gil, G., López-Fernández, A., Artegiani, B., Wasielewska, J. M., Lee, C.-C., Lippert, M. T., Kempermann, G., Takagaki, K. and Calegari, F. (2020). Increasing neurogenesis refines hippocampal activity rejuvenating navigational learning strategies and contextual memory throughout life. *Nat. Commun.* **11**, 135. doi:10.1038/s41467-019-14026-z

Bettio, L. E. B., Rajendran, L. and Gil-Mohapel, J. (2017). The effects of aging in the hippocampus and cognitive decline. *Neurosci. Biobehav. Rev.* **79**, 66-86. doi:10.1016/j.neubiorev.2017.04.030

Brandhorst, S., Choi, I. Y., Wei, M., Cheng, C. W., Sedrakyan, S., Navarrete, G., Dubeau, L., Yap, L. P., Park, R., Vinciguerra, M. et al. (2015). A periodic diet that mimics fasting promotes multi-system regeneration, enhanced cognitive performance, and healthspan. *Cell Metab.* **22**, 86-99. doi:10.1016/j.cmet.2015.05.012

Campos, L. S., Leone, D. P., Relvas, J. B., Brakebusch, C., Fässler, R., Suter, U. and Ffrench-Constant, C. (2004). β1 integrins activate a MAPK signalling pathway in neural stem cells that contributes to their maintenance. *Development* **131**, 3433-3444. doi:10.1242/dev.01199

Cembrowski, M. S., Wang, L., Sugino, K., Shields, B. C. and Spruston, N. (2016). Hipposeq: a comprehensive RNA-seq database of gene expression in hippocampal principal neurons. *Elife* **5**, e14997. doi:10.7554/eLife.14997

Charvet, C. J. and Finlay, B. L. (2018). Comparing adult hippocampal neurogenesis across species: translating time to predict the tempo in humans. *Front. Neurosci.* **12**, 706. doi:10.3389/fnins.2018.00706

Colantuoni, C., Lipska, B. K., Ye, T., Hyde, T. M., Tao, R., Leek, J. T., Colantuoni, E. A., Elkahloun, A. G., Herman, M. M., Weinberger, D. R. et al. (2011). Temporal dynamics and genetic control of transcription in the human prefrontal cortex. *Nature* **478**, 519-523. doi:10.1038/nature10524

Galfrè, S. G., Morandin, F., Pietrosanto, M., Cremisi, F. and Helmer-Citterich, M. (2021). COTAN: scRNA-seq data analysis based on gene co-expression. *NAR Genom. Bioinform.* **3**, lqab072. doi:10.1093/nargab/lqab072

Gonçalves, J. T., Schafer, S. T. and Gage, F. H. (2016). Adult neurogenesis in the hippocampus: from stem cells to behavior. *Cell* **167**, 897-914. doi:10.1016/j.cell.2016.10.021

Grove, E. A. and Tole, S. (1999). Patterning events and specification signals in the developing hippocampus. *Cereb. Cortex* **9**, 551-561. doi:10.1093/cercor/9.6.551

Grove, E. A., Tole, S., Limon, J., Yip, L. and Ragsdale, C. W. (1998). The hem of the embryonic cerebral cortex is defined by the expression of multiple Wnt genes and is compromised in Gli3-deficient mice. *Development* **125**, 2315-2325. doi:10.1242/dev.125.12.2315

Hall, M. L., Givens, S., Santosh, N., Iacovino, M., Kyba, M. and Ogle, B. M. (2022). Laminin 411 mediates endothelial specification via multiple signaling axes that converge on β-catenin. *Stem Cell Rep.* **17**, 569-583. doi:10.1016/j.stemcr.2022.01.005

Horejs, C.-M., Serio, A., Purvis, A., Gormley, A. J., Bertazzo, S., Poliniewicz, A., Wang, A. J., DiMaggio, P., Hohenester, E. and Stevens, M. M. (2014). Biologically-active laminin-111 fragment that modulates the epithelial-to-mesenchymal transition in embryonic stem cells. *Proc. Natl. Acad. Sci. USA* **111**, 5908-5913. doi:10.1073/pnas.1403139111

Hyysalo, A., Ristola, M., Mäkinen, M. E.-L., Häyrynen, S., Nykter, M. and Narkilahti, S. (2017). Laminin α5 substrates promote survival, network formation and functional development of human pluripotent stem cell-derived neurons in vitro. *Stem Cell Res.* **24**, 118-127. doi:10.1016/j.scr.2017.09.002

Imayoshi, I., Sakamoto, M., Yamaguchi, M., Mori, K. and Kageyama, R. (2010). Essential roles of Notch signaling in maintenance of neural stem cells in developing and adult brains. *J. Neurosci.* **30**, 3489-3498. doi:10.1523/JNEUROSCI.4987-09.2010

Inta, D., Cameron, H. A. and Gass, P. (2015). New neurons in the adult striatum: from rodents to humans. *Trends Neurosci.* **38**, 517-523. doi:10.1016/j.tins.2015.07.005

Iwano, T., Masuda, A., Kiyonari, H., Enomoto, H. and Matsuzaki, F. (2012). Prox1 postmitotically defines dentate gyrus cells by specifying granule cell identity over CA3 pyramidal cell fate in the hippocampus. *Development* **139**, 3051-3062.

Kiritsi, D., Has, C. and Bruckner-Tuderman, L. (2013). Laminin 332 in junctional epidermolysis bullosa. *Cell Adh. Migr.* **7**, 135-141. doi:10.4161/cam.22418

Knoth, R., Singec, I., Ditter, M., Pantazis, G., Capetian, P., Meyer, R. P., Horvat, V., Volk, B. and Kempermann, G. (2010). Murine Features of Neurogenesis in the Human Hippocampus across the Lifespan from 0 to 100 Years. *PLoS One* **5**, e8809. doi:10.1371/journal.pone.0008809

Lavado, A., Lagutin, O. V., Chow, L. M. L., Baker, S. J. and Oliver, G. (2010). Prox1 is required for granule cell maturation and intermediate progenitor maintenance during brain neurogenesis. *PLoS Biol.* **8**, e1000460. doi:10.1371/journal.pbio.1000460

Lee, S. M., Tole, S., Grove, E. and McMahon, A. P. (2000). A local Wnt-3a signal is required for development of the mammalian hippocampus. *Development* **127**, 457-467. doi:10.1242/dev.127.3.457

Lester, A. W., Moffat, S. D., Wiener, J. M., Barnes, C. A. and Wolbers, T. (2017). The aging navigational system. *Neuron* **95**, 1019-1035. doi:10.1016/j.neuron.2017.06.037

Long, K. R. and Huttner, W. B. (2019). How the extracellular matrix shapes neural development. *Open Biol.* **9**, 180216. doi:10.1098/rsob.180216

Long, K., Moss, L., Laursen, L., Boulter, L. and Ffrench-Constant, C. (2016). Integrin signalling regulates the expansion of neuroepithelial progenitors and neurogenesis via Wnt7a and Decorin. *Nat. Commun.* **7**, 10354. doi:10.1038/ncomms10354

Lugert, S., Basak, O., Knuckles, P., Haussler, U., Fabel, K., Götz, M., Haas, C. A., Kempermann, G., Taylor, V. and Giachino, C. (2010). Quiescent and active hippocampal neural stem cells with distinct morphologies respond selectively to physiological and pathological stimuli and aging. *Cell Stem Cell* **6**, 445-456. doi:10.1016/j.stem.2010.03.017

Ma, W., Tavakoli, T., Derby, E., Serebryakova, Y., Rao, M. S. and Mattson, M. P. (2008). Cell-extracellular matrix interactions regulate neural differentiation of human embryonic stem cells. *BMC Dev. Biol.* **8**, 90. doi:10.1186/1471-213X-8-90

Machon, O., Backman, M., Machonova, O., Kozmik, Z., Vacik, T., Andersen, L. and Krauss, S. (2007). A dynamic gradient of Wnt signaling controls initiation of neurogenesis in the mammalian cortex and cellular specification in the hippocampus. *Dev. Biol.* **311**, 223-237. doi:10.1016/j.ydbio.2007.08.038

Martins, M., Galfrè, S., Terrigno, M., Pandolfini, L., Appolloni, I., Dunville, K., Marranci, A., Rizzo, M., Mercatanti, A., Poliseno, L. et al. (2021). A eutherian-specific microRNA controls the translation of Satb2 in a model of cortical differentiation. *Stem Cell Rep.* **16**, 1496-1509. doi:10.1016/j.stemcr.2021.04.020

Ming, G. and Song, H. (2011). Adult neurogenesis in the mammalian brain: significant answers and significant questions. *Neuron* **70**, 687-702. doi:10.1016/j.neuron.2011.05.001

Mitchelmore, C., Kjaerulff, K. M., Pedersen, H. C., Nielsen, J. V., Rasmussen, T. E., Fisker, M. F., Finsen, B., Pedersen, K. M. and Jensen, N. A. (2002). Characterization of two novel nuclear BTB/POZ domain zinc finger isoforms. Association with differentiation of hippocampal neurons, cerebellar granule cells, and macroglia. *J. Biol. Chem.* **277**, 7598-7609. doi:10.1074/jbc.M110023200

Nakashima, Y. and Omasa, T. (2016). What kind of signaling maintains Pluripotency and viability in human-induced pluripotent stem cells cultured on Laminin-511 with serum-free medium? *BioResearch Open Access* **5**, 84-93. doi:10.1089/biores.2016.0001

Nascimento, M. A., Sorokin, L. and Coelho-Sampaio, T. (2018). Fractone bulbs derive from ependymal cells and their laminin composition influence the stem cell niche in the subventricular zone. *J. Neurosci.* **38**, 3880-3889. doi:10.1523/JNEUROSCI.3064-17.2018

Naujok, O., Lentes, J., Diekmann, U., Davenport, C. and Lenzen, S. (2014). Cytotoxicity and activation of the Wnt/beta-catenin pathway in mouse embryonic stem cells treated with four GSK3 inhibitors. *BMC Res. Notes* **7**, 273. doi:10.1186/1756-0500-7-273

Ni, Y., Liu, B., Wu, X., Liu, J., Ba, R. and Zhao, C. (2021). FOXG1 directly suppresses Wnt5a during the development of the hippocampus. *Neurosci. Bull.* **37**, 298-310. doi:10.1007/s12264-020-00618-z

Nielsen, J. V., Thomassen, M., Møllgård, K., Noraberg, J. and Jensen, N. A. (2014). Zbtb20 defines a hippocampal neuronal identity through direct repression of genes that control projection neuron development in the isocortex. *Cereb. Cortex* **24**, 1216-1229. doi:10.1093/cercor/bhs400

Nirwane, A. and Yao, Y. (2019). Laminins and their receptors in the CNS: Laminins and their receptors in the CNS. *Biol. Rev.* **94**, 283-306. doi:10.1111/brv.12454

Noguchi, H., Castillo, J. G., Nakashima, K. and Pleasure, S. J. (2019). Suppressor of fused controls perinatal expansion and quiescence of future dentate adult neural stem cells. *Elife* **8**, e42918. doi:10.7554/eLife.42918

Palmer, T. D., Willhoite, A. R. and Gage, F. H. (2000). Vascular niche for adult hippocampal neurogenesis. *J. Comp. Neurol.* **425**, 479-494. doi:10.1002/1096-9861(20001002)425:4<479::AID-CNE2>3.0.CO;2-3

Patro, R., Duggal, G., Love, M. I., Irizarry, R. A. and Kingsford, C. (2017). Salmon provides fast and bias-aware quantification of transcript expression. *Nat. Methods* **14**, 417-419. doi:10.1038/nmeth.4197

Pencea, V., Bingaman, K. D., Freedman, L. J. and Luskin, M. B. (2001). Neurogenesis in the subventricular zone and rostral migratory stream of the neonatal and adult primate forebrain. *Exp. Neurol.* **172**, 1-16. doi:10.1006/exnr.2001.7768

Quattrocolo, G., Fishell, G. and Petros, T. J. (2017). Heterotopic transplantations reveal environmental influences on interneuron diversity and maturation. *Cell Rep.* **21**, 721-731. doi:10.1016/j.celrep.2017.09.075

Rosenthal, E. H., Tonchev, A. B., Stoykova, A. and Chowdhury, K. (2012). Regulation of archicortical arealization by the transcription factor Zbtb20. *Hippocampus* **22**, 2144-2156. doi:10.1002/hipo.22035

Sakaguchi, H., Kadoshima, T., Soen, M., Narii, N., Ishida, Y., Ohgushi, M., Takahashi, J., Eiraku, M. and Sasai, Y. (2015). Generation of functional hippocampal neurons from self-organizing human embryonic stem cell-derived dorsomedial telencephalic tissue. *Nat. Commun.* **6**, 8896. doi:10.1038/ncomms9896

Sarkar, A., Mei, A., Paquola, A. C. M., Stern, S., Bardy, C., Klug, J. R., Kim, S., Neshat, N., Kim, H. J., Ku, M. et al. (2018). Efficient generation of CA3 neurons from human pluripotent stem cells enables modeling of hippocampal connectivity in vitro. *Cell Stem Cell* **22**, 684-697.e9. doi:10.1016/j.stem.2018.04.009

Sasaki, T., Takagi, J., Giudici, C., Yamada, Y., Arikawa-Hirasawa, E., Deutzmann, R., Timpl, R., Sonnenberg, A., Bächinger, H. P. and Tonge, D. (2010). Laminin-121—recombinant expression and interactions with integrins. *Matrix Biol.* **29**, 484-493. doi:10.1016/j.matbio.2010.05.004

Shi, Y., Kirwan, P., Smith, J., Robinson, H. P. C. and Livesey, F. J. (2012a). Human cerebral cortex development from pluripotent stem cells to functional excitatory synapses. *Nat. Neurosci.* **15**, 477-486. doi:10.1038/nn.3041

Shi, Y., Kirwan, P. and Livesey, F. J. (2012b). Directed differentiation of human pluripotent stem cells to cerebral cortex neurons and neural networks. *Nat. Protoc.* **7**, 1836-1846. doi:10.1038/nprot.2012.116

Simon, R., Brylka, H., Schwegler, H., Venkataramanappa, S., Andratschke, J., Wiegreffe, C., Liu, P., Fuchs, E., Jenkins, N. A., Copeland, N. G. et al. (2012). A dual function of Bcl11b/Ctip2 in hippocampal neurogenesis. *EMBO J.* **31**, 2922-2936. doi:10.1038/emboj.2012.142

Song, J., Sun, J., Moss, J., Wen, Z., Sun, G. J., Hsu, D., Zhong, C., Davoudi, H., Christian, K. M., Toni, N. et al. (2013). Parvalbumin interneurons mediate neuronal circuitry–neurogenesis coupling in the adult hippocampus. *Nat. Neurosci.* **16**, 1728-1730. doi:10.1038/nn.3572

Terrigno, M., Busti, I., Alia, C., Pietrasanta, M., Arisi, I., D'Onofrio, M., Caleo, M. and Cremisi, F. (2018). Neurons generated by mouse ESCs with hippocampal or cortical identity display distinct projection patterns when co-transplanted in the adult brain. *Stem Cell Rep.* **10**, 1016-1029. doi:10.1016/j.stemcr.2018.01.010

Urbán, N. and Guillemot, F. (2014). Neurogenesis in the embryonic and adult brain: same regulators, different roles. *Front. Cell. Neurosci.* **8**, 396. doi:10.3389/fncel.2014.00396

van Praag, H., Shubert, T., Zhao, C. and Gage, F. H. (2005). Exercise enhances learning and hippocampal neurogenesis in aged mice. *J. Neurosci.* **25**, 8680-8685. doi:10.1523/JNEUROSCI.1731-05.2005

Xie, Z., Ma, X., Ji, W., Zhou, G., Lu, Y., Xiang, Z., Wang, Y. X., Zhang, L., Hu, Y., Ding, Y.-Q. et al. (2010). Zbtb20 is essential for the specification of CA1 field identity in the developing hippocampus. *Proc. Natl. Acad. Sci. USA* **107**, 6510-6515. doi:10.1073/pnas.0912315107

Yu, D. X., Di Giorgio, F. P., Yao, J., Marchetto, M. C., Brennand, K., Wright, R., Mei, A., McHenry, L., Lisuk, D., Grasmick, J. M. et al. (2014a). Modeling hippocampal neurogenesis using human pluripotent stem cells. *Stem Cell Rep.* **2**, 295-310. doi:10.1016/j.stemcr.2014.01.009

Yu, D. X., Marchetto, M. C. and Gage, F. H. (2014b). How to make a hippocampal dentate gyrus granule neuron. *Development* **141**, 2366-2375. doi:10.1242/dev.096776